

Use Authorization

In presenting this thesis in partial fulfillment of the requirements for an advanced degree at Idaho State University, I agree that the Library shall make it freely available for inspection. I further state that permission to download and/or print my thesis for scholarly purposes may be granted by the Dean of the Graduate School, Dean of my academic division, or by the University Librarian. It is understood that any copying or publication of this thesis for financial gain shall not be allowed without my written permission.

Signature _____

Date _____

THE DESIGN OF A RADIOISOTOPIC THERMOELECTRIC GENERATOR
POWERED BY STRONTIUM-90

by

Micah Kingston

A thesis

Submitted in partial fulfillment

Of the requirements for the degree of

Master of Engineering in the Department of

Nuclear Engineering and Health Physics

Idaho State University

Fall 2014

Committee Approval

Thesis of Micah Kinston

To the Graduate Faculty:

The members of the committee appointed to examine the thesis of Micah Kingston find it satisfactory and recommend that it be accepted.

Jay Kunze, PhD.

Major Advisor

Chad Pope, PhD.

Committee Member

Seyed H. Mousavinezhad, PhD.

Graduate Faculty Representative

Acknowledgements

I would like to acknowledge my family, whose patience and support were essential for me to finish the degree.

I would also like to acknowledge Dr. Jay Kunze, who was instrumental in providing a path to graduation, who consistently places the welfare of the students above his own. It was a tremendous joy to work under and gain insight from the living legend that is Dr. Kunze.

I would also like to acknowledge Dr. Chad Pope, whose talents and teaching ability are matched only by his desire to help those around him. Thank you for your guidance and continuous respect.

Table of Contents

List of Figures	vi
List of Tables	viii
Glossary	ix
Abstract	x
Chapter 1 – Introduction and Background.....	1
Options in Dealing with Spent Nuclear Fuel (SNF)	3
Composition of Spent Nuclear Fuel (SNF).....	4
An Application for Sr-90	4
Sr-90 Separation Techniques	6
Sr-90 Material Composition for RTG.....	7
SrTiO ₃ Fuel Fabrication	7
Russian Use of Sr-90 RTG's.....	9
Sr-90 Vs. Pu-238 RTG.....	10
Application for Study.....	13
Chapter 2 - Design Criteria	17
Sr-90TiO ₃ as a Heat Source for an RTG.....	17
Shielding	21
Shielding: Dealing with Bremsstrahlung Radiation	21
Shielding: β^- Particle Range	27
Shielding: Calculating Buildup Factor.....	28
Shielding: Calculating Thickness	30
Shielding: Choice of Shielding Material.....	40
Dealing with the Heat	42
Dealing with the Heat of the Fuel Cell	42

Dealing with the Heat of the Intermediate Layers of the Power Unit	44
Dealing with the Heat through Proper Thermocouple Design.....	44
Dealing with the Heat at the Outer Layer of the Power Unit.....	49
Dealing with the Heat Using Al Encasing and Heat Dissipation Fins.....	50
Possible Manufacturing Challenges.....	61
Safety Considerations – Risk of Terrorism.....	62
Safety Considerations – Dealing with a Non-Load	63
Safety Considerations – Transportation, Maintenance, and Disposal	64
Chapter 3 - Specific Design	66
Optimization of Surface Area to Maximize Amount of Thermocouples Used	66
Surface Area for the Side of the Shielded Fuel Cell Cylinder	68
Maximizing the Number of Thermocouples on the Shielded Fuel Cell Top and Bottom.....	
Attempting to Achieve 7% efficiency.....	72
Appropriate Shielding for a Product Sold to the Public	72
Not Destroying Itself with no Load	73
Adding Side Fins to Design for Power Unit in Standing Air	78
Chapter 4 - Marketing.....	81
Possible Uses of the Technology	81
Ideal Application.....	82
Future Work	83
Chapter 5 - Conclusion	85
References.....	86
Appendix A – Excel 2007 Code used to solve the # of squares in a circle	89

List of Figures

Fig. 1 Flow chart showing process of forming SrTiO ₃ from separated Sr-90 in the form of SrCO ₃	9
Fig. 2. Complete decay chain of Sr-90	11
Fig. 3. Complete decay chain of Pu-238.....	12
Fig. 4. Off grid DC (left) and AC (right) with optional generator solar power system	15
Fig. 5. Illustration of Bremsstrahlung Radiation	22
Fig. 6. Illustration of radiation buildup avoided (left) and occurring in material (right)..	29
Fig. 7. Linear attenuation coefficient for Pb vs. photon energy.	30
Fig. 8. Illustration of cylindrical fuel cell with a shield and variable labels.....	32
Fig. 9a. Parameter m vs. A/R	36
Fig. 9b. Function of cylinder self absorption exponent divided by $m \frac{\mu_s z}{m}$	36
Fig. 10a. $F(\theta, b_2)$ vs b_2 for $b_2 = 0$ to 8	37
Fig. 10b. $F(\theta, b_2)$ vs b_2 for $b_2 = 8$ to 15	37
Fig. 10c. $F(\theta, b_2)$ vs b_2 for $b_2 = 16$ to 24	37
Fig. 10d. $F(\theta, b_2)$ vs b_2 for $b_2 = 24$ to 31	37
Fig. 11. Specific gamma ray constants $\left[\frac{Rm^2}{hrCi} \right]$ or $\left[R \text{ at } \frac{1m}{hrCi} \right]$ and conversion factors	38
Fig. 12. Fuel cylinder self-absorption exponent $\mu_s z$ as a function of $\mu_s R$ for $\frac{a}{R} \geq 10$	39
Fig. 13. Illustration of a functioning thermocouple	46
Fig. 14. Exploded view of the thermocouple used in RTG design	47
Fig. 15. Illustration of a heat dissipation fin and variables used to represent its dimensions.....	51
Fig. 16. Top view illustration of the layers of the power unit	57
Fig. 17. Top view illustration of the layers of the power unit designed for standing air..	60

Fig. 18. Illustration of array of the thermocouple hot junctions on surface	67
of shielded fuel cell	
Fig. 19. Illustration of a single “switch rod” (left) and the “switch rod ring”	74
(right) installed (in off position)	
Fig. 20. Illustration of the hot and cold junction of a single thermocouple	75
Fig. 21. Top view of hot and cold thermocouple junctions connected	76
Fig. 22. “X-Ray” view of Sr-90TiO ₃ power unit and its components	76
Fig. 23. 3-D rendition of Sr-90TiO ₃ power unit (designed to be maintained under a constant breeze)	79
Fig. 24. 3-D rendition of Sr-90TiO ₃ power unit (designed to be in standing air)	80
Fig. 25. Illustration of DC (left) and AC (right) remote power system using a single	83
Sr-90TiO ₃ power unit	
Fig. 26. Illustration of AC remote power system using multiple Sr-90TiO ₃	83
power units	

List of Tables

Table 1. Energy consumption for common household appliances	14
Table 2a. Table of average Bremsstrahlung energy produced per beta particle	23
release for Sr-90 (left) and Y-90 (right)	
Table 2b. Verification of average Bremsstrahlung energy produced per beta for Sr-90 ..	25
Table 2c. Verification of average Bremsstrahlung energy produced per beta for Sr-90 ..	26
Table 3. Thicknesses, figure values, and corresponding dose rates investigated	40
Table 4. Shielding thicknesses and mass of U, Pb, and Fe	42
Table 5. Thermocouple components with effective conductivity coefficient.....	49
Table 6. Layer descriptions, conductivities, and temperatures of power unit	56
Table 7. Layer descriptions, conductivities, and temperatures of power unit designed for standing air	59
Table 8. Melting points of considered materials.....	77

Glossary

Thermal Energy Neutrons: Neutrons at room temperatures usually at around 0.025 eV average energy.

Spent Nuclear Fuel (SNF): Nuclear fuel that has been “burned” within a nuclear power plant, depleting the fissile material.

Nuclear Material: A material that is either fissile or fertile.

Fissile Material: A material that when a thermal neutron is absorbed by the material, it undergoes fission.

Fertile Material: A material that when a neutron is absorbed by the material, it transmutes to a fissile material.

Fission: The process by which a material absorbs a neutron and breaks apart, releasing energy, particles, and fission products.

Fission Products: A byproduct of a fission reaction. Usually consists of an element roughly half the mass of the fissioned material, which are often radioactive themselves. Examples include Sr-90, I-131, and Cs-137.

Light Water Reactors (LWRs): Nuclear power reactors that use regular water as a coolant and a moderator.

Bremsstrahlung Radiation: Also referred to as: “braking radiation”, produced by the slowing down of electrons that pass through the electron cloud of an atom and are attracted to the nucleus of said atom enough to alter the trajectory of the incoming electron.

Secular Equilibrium: The situation that occurs when the half-life of a daughter radionuclide is much shorter than the parent radionuclide. This results in the equivalent half-life of the parent and daughter radionuclides to be approximately equal to the half-life of the parent radionuclide.

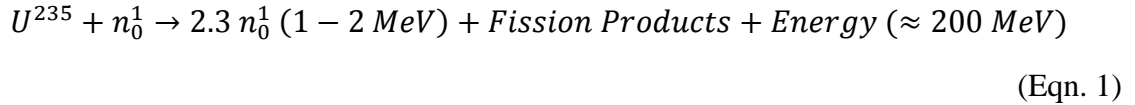
Abstract

There are currently 99 nuclear power plants that are in operation in the United States which produce approximately 20 metric tons of spent nuclear fuel and approximately 200 metric tons of depleted Uranium per nuclear power plant per year. One of the possible solutions to deal with the increasing amount of spent nuclear fuel and depleted Uranium is to reprocess the fuel (breeder reactors use depleted Uranium). In addition to being able to re-use the fertile and fissile materials, it is also possible to use some of the fission products in a productive way. One such fission product is Strontium-90 (Sr-90) which is a pure beta emitter with a 28.78 year half life that decays to stable and non-toxic Zirconium-90. A power unit using the radionuclide Sr-90 was designed to produce 300 W of electricity after 30 years of use (621 W initially). The power unit's fuel cell consists of Sr-90TiO₃ because the chemical, thermal, and physical properties were ideal compared to other Sr-90 compounds. A power unit was designed to be standing under a breeze (or the use of cooling fans) and in the case of the power unit not experiencing any external forced convection. The specifications for the latter case are described here. The unit itself weighs approximately 582.5 lbs (108.7 lbs are depleted Uranium) and has 29 heat dissipation fins that are 15.0 cm x 1.0 cm x 87.46 cm. Each heat dissipation fin has 50 side fins that are 1.15 cm x 0.2 cm x 87.46 cm. The fuel cell has a cylindrical shape and a radius of 4.5 cm and a height of 72.0 cm. The dose rate that an individual would receive touching the outside of the prime surface (the base of the heating fins) is by standing 1 m away from the power unit is 0.44×10^{-6} Rem/hr (0.0044 μ Gy/hr). The Sr-90TiO₃ power unit was designed to be fully functional without any moving parts and provides a sustainable use for an abundant fission product, as well as an effective way to use some of the depleted Uranium that is stockpiled throughout the United States.

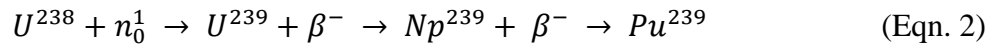
Chapter 1 – Introduction and Background

When nuclear power is produced in light water reactors (LWRs), it is by using primarily neutrons at thermal energies (approximately 0.025 eV) and Uranium (U). Natural U consists of U^{235} (0.72%) which is a fissile material, meaning adding a neutron to the material will cause fission, and U^{238} (99.28%) which is a fertile material, meaning adding a neutron to the material will cause the material to become fissile (eventually Pu-239). There are two primary reactions that occur within the nuclear power plant, fission and neutron capture. Each are described by Eqns. 1 and 2 respectively. After the neutron capture reaction occurs there can be a second fission reaction described by Eqn. 3 shown below.

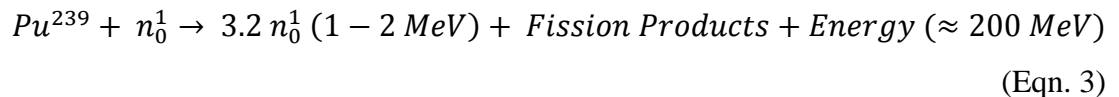
Fission using U^{235}



Neutron Capture with U^{238}



Fission using Pu^{239}



During the process of fission within a nuclear power plant, heat and radiation are released turning water into steam which turns a turbine and produces electricity. New fuel consists of between 3% - 5% fissile material and the rest is U^{238} . During each fueling cycle some of the fertile material is turned into fissile material and most of the fissile material is “burned” until the fuel consists of between 1% - 2% fissile materials, where approximately 6% of the total original Uranium has been consumed. Each fueling cycle lasts for approximately 18 or 24 months. At the end of the fueling cycle the fuel is considered to be spent nuclear fuel (SNF).

Each of the nuclear power plants in the United States produces approximately 20 metric tons of SNF per year and with 99 nuclear power plants currently in operation in the United States today, we are creating approximately 1,980 metric tons of SNF annually (Bruno & Ewing 2006). Deciding what to do with the SNF has been hotly debated over the past few decades. Most everyone can agree that something should be done with the SNF, but few agree on what solution should be pursued and even less have any interest in the execution of that solution to be anywhere close to the location in which they reside. This has resulted in doing nothing to solve the long-term problem. In the short-term, America’s nuclear power industry has been tasked with the use of interim storage methods and are currently required to keep all SNF on the property of each respective nuclear power plant.

Options in Dealing with Spent Nuclear Fuel (SNF)

There are three basic options on what to do with SNF: reprocess or recycle it, find a long-term storage location with the expectation that the SNF will be stored in that location for thousands of years, or continue doing what we are doing now, which is to temporarily store the SNF onsite at the nuclear power plants until a long-term solution can be determined. This means that there are really only two long-term solutions on dealing with SNF, permanent long-term storage or reprocessing. There are advantages and challenges to each option. For the long-term storage option, one of the biggest challenges of having a long-term storage location for the SNF is the fact that the local population usually holds the opinion of “Not In My Back Yard”, or NIMBY. A secondary problem often mentioned by anti-nuclear activists is that it is impossible to design a facility to house the nuclear materials safely for thousands of years. To resolve this issue for the use of long-term storage the real solution would be to design and build the facility that has a continuous maintenance and security program.

Regarding the option of commercially reprocessing the SNF, there are a few challenges. The first challenge is that even if reprocessing is done, there is still a need for a repository because there are wastes created while reprocessing the SNF (Todd 2008). Another challenge is when separating the fissile and fertile materials from the fission products it is possible to separate out the Plutonium, which presents an increased risk of proliferation of nuclear weapons. If such a task may be too high of a security risk to be performed by a private company, it may be prudent to have assistance from the military or government funded Department of Energy laboratories such as Sandia National Laboratories, or Idaho National Laboratories. However, it can also be said that leaving the

Plutonium in the SNF casks un-separated and on the property of the nuclear power plants also presents a risk of proliferation; making it more beneficial to extract and consume the Plutonium by “burning” it in a nuclear reactor in the short term rather than store it in the long term (Hippel 2001).

A challenge to that argument is that at the current prices of Uranium and the Uranium fuel rods, it is actually cheaper to produce new fuel, use it once, and store it than it is to reprocess the SNF (Bun et al 2003). However, it may be prudent to have the government make up the difference of the market in the short term so that the full potential of Uranium as a power source can be realized through next generation options such as the breeder reactor, which can “burn” 100% of Uranium, which under the current supply of already mined Uranium within the United States could fuel America’s energy needs for over 1000 years, if the required infrastructure was allowed to be setup. Another benefit of reprocessing is that there may be other uses for some of the fission products that may help reprocessing to become more economically viable.

Composition of Spent Nuclear Fuel (SNF)

The SNF that has been taken out of a typical nuclear reactor and after about 10 years of storage is approximately 95.6% Uranium, 2.9% stable (decayed) fission products, 0.9 % various isotopes of Plutonium, 0.3% Cesium (Cs) and Strontium (Sr), 0.1% long lived Iodine and Technetium, 0.1% minor Actinides, and 0.1% other long lived fission products. Most of the radiotoxicity of the SNF is due to the long lived fission products and the minor actinides, which can be separated and transmuted in fast spectrum reactors

or disposed of in much smaller containers than the SNF (Todd 2008). Most of the heat production from 30 yr old (or younger) SNF is from Cs and Sr. Cs-137 (30yr, 6.2% yield) can be effectively used for food irradiation facilities, and other uses requiring sterilization from bacteria and viruses.

An Application for Sr-90

Sr-90 (28.8 yr, 5.2 % yield) may be ideal for a heat source for multiple reasons. First of all, immediately after the SNF is taken out of a typical nuclear reactor, Sr-90 constitutes 5.75% of the fission products produced. With 99 nuclear power plants in the U.S. each producing 20 metric tons of SNF per year, and the ability to recover as much as 98% of the Sr-90 from the SNF (Shor et al 1971), it means that the United States has the potential of producing 5.15 metric tons of Sr-90 each year, which represents 7.1×10^8 Curies of Sr-90.

Sr-90 is also a pure beta-emitter and is in secular equilibrium with Yttrium-90 (Y-90), another pure beta-emitter. The half-life of Sr-90 is 28.79 years, so one has the opportunity of using this heat source for a very long time. When Sr-90 and Y-90 decay, the maximum energy released is 0.546 MeV and 2.28 MeV respectively (the average energy released is 0.182 MeV and 0.760 MeV respectively). However, there is one drawback to this high energy release, which is that the energy of the β^- s of Sr-90 and Y-90 are high enough to cause Bremsstrahlung radiation during the process of slowing down the β^- s and must be dealt with appropriately. The energy density of Sr-90 (0.916 Wth/g) suggests that it may be a viable option in the design of a radio-isotopic thermo-electric

generator (RTG). Units have actually been built by Oak Ridge National Labs (ORNL) in the late 1950's and by the Russians in the 1970's (Shore et al 1971, Sneve 2007).

Sr-90 Separation Techniques

Before Sr-90 can be used in an RTG it must first be separated from the SNF. In 1948, Oak Ridge National Laboratories (ORNL) began using resins in an ion-exchange system to separate many of the fission products. But the ion-exchange system was replaced with precipitation processes due to the high radiation degradation of the resins (Shor et al 1971). By 1958 ORNL had finished the Fission Products Development Laboratory (FPDL) and was able to more aggressively investigate separation techniques. By 1960, ORNL produced 7kCi of Sr-90 using precipitation processes.

In 1953 Hanford also began working on fission-product separation. Once the first large scale purification process was finished at the Fission Products Development Laboratory (FPDL), production of Sr-90 was transferred to Hanford. Once there, Hanford used a PbSO_4 carrier precipitation and ion exchange method to purify 75 kCi of Sr-90 between the months of August 1960 to February 1961. Over the next four years Hanford went on to separate over 8 MCi of Sr-90 (Shor et al 1971). From there, Sr-90 fuel material compositions were explored by ORNL.

Sr-90 Material Composition for RTG

There were a number of different chemical forms of Sr-90 that were considered by ORNL for the use in an RTG. The three main factors in making the appropriate choice were energy density of the material, thermal stability, and solubility in water. The top five materials considered were: SrTiO_3 , SrF_2 , SrO , Sr , and Sr_2TiO_4 . SrO and SrTiO_3 were the top two materials considered. The biggest advantage for SrO was its energy density, but because it was soluble in water, this increased the chances for radionuclide leakage; therefore SrTiO_3 was chosen (Shor et al 1971). SrTiO_3 has a melting point of 2040°C , making it ideal for a high temperature RTG. For this investigation, all calculations and simulations will be done under the assumption that SrTiO_3 was the material used.

SrTiO_3 Fuel Fabrication

Once the SrTiO_3 powder was formed there were three methods investigated by ORNL on how to fabricate the fuel pellets. The first method is known as cold-forming, which is a process of compacting a powder inside a metal die usually by some type of hydraulic press inside a hot cell. However, the dimensional control and reproducibility have been found to be relatively low (Shor et al 1971).

The second method was known as hot-forming, which is similar to the cold-forming process, except heat and time was added. It was found that the most consistent dimensions and density of the fuel pellet came about when the pellet was pressed for 5 minutes at 5,000 – 10,000 psi (depending on the size of the pellet). The pellet was then removed, inverted, and pressed again for another 5 minutes at the same pressure (Shor et

al 1971). This process was reported to be more difficult than the cold-forming method but it received much more consistency in the pellet quality.

The third method that was explored is known as melt-casting, which is simply heating the powder for a time. Melt-casting was the least effective method of the three. For this investigation it was assumed that the hot-forming method would be used in the fabrication of a Sr-90TiO₃ power unit. Regardless of the method used by ORNL was to form the fuel pellet, the next step was to sinter the fuel pellets at 1400 °C for 8 hours. The rate at which the sintering furnace was heated and cooled was 100 °C/hr. It is also common practice to make a cylindrical fuel pellet with a diameter to height ratio of 2:1. The entire process used to bring the separated Sr-90 to SrTiO₃ fuel pellets is illustrated in Fig. 1.

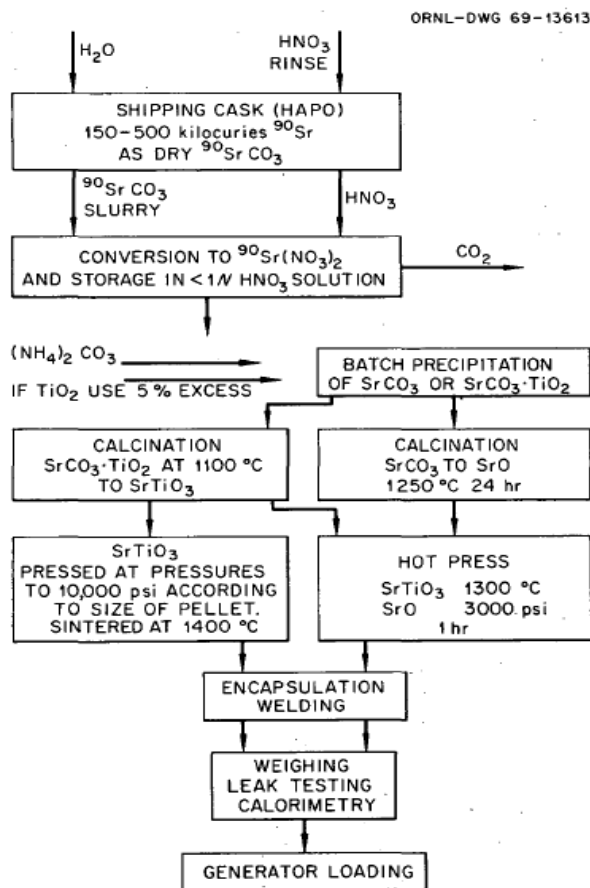


Fig. 1. Flow chart showing process of forming SrTiO₃ from separated Sr-90 in the form of SrCO₃ (Shor et al 1971).

Russian Use of Sr-90 RTG's

The Russians built more than 1000 Sr-90 RTG's in the late 1970's and have over 650 Sr-90 RTG's in use as of 2006. The Russians produced four types of Sr-90 RTG that ranged in weight and activity from 565 kg to 2300 kg, 35 kCi to 340 kCi (at the time of production) respectively. Just as ORNL, the Russians used a SrTiO₃ material for the fuel component of the RTG. They also organized a decommissioning project (organized in part by the Norwegian government) for any RTG's still in use and tracked the status of each RTG and plans on the time of required decommissioning (Sneve 2007).

Sr-90 Vs. Pu-238 RTG

For many familiar with the space program an obvious question might come up: “Why use Sr-90 as the fuel for the RTG instead of Pu-238, which is used in the space probes to date?” Pu-238 certainly is the radionuclide that is most commonly used as the fuel for the RTGs used in the American space program. It is likely that Pu-238 was chosen by the space program because Pu-238 has a half-life of 87.4 years. However, the half-life of a nuclide is not the only thing to consider when designing an RTG that can be used by the general public. Pu-238 is a nuclear material that has a long decay chain that includes Radon-222 and would release Radon gas into the environment and the surrounding area. It could build up around the device causing an unnecessary health concern to the public and the customer. Sr-90 has only solid materials in its decay chain which eliminates the possibility of radioactive gases leaking from the device, which is a concern for the Pu-238 powered RTG.

Radioactive gases are not the only concern with the Pu-238 decay chain. There are also solid radioactive elements in the Pu-238 decay chain such as U-234, Ra-226, Po-218, Pb-214, Bi-214, Po-214, Pb-210, Bi-210, and Po-210 all of which are toxic due to its radioactivity and its chemical properties. For example, the Pu-238 decay chain has multiple isotopes of lead (Pb), a heavy metals that if exposed to humans can cause serious illness such as nervous system damage, kidney damage, liver damage, and other ailments. An illustration of the complete decay chain for Sr-90 and Pu-238 are shown in Fig. 2 and Fig. 3 respectively.

Sr – 90 Decay Chain

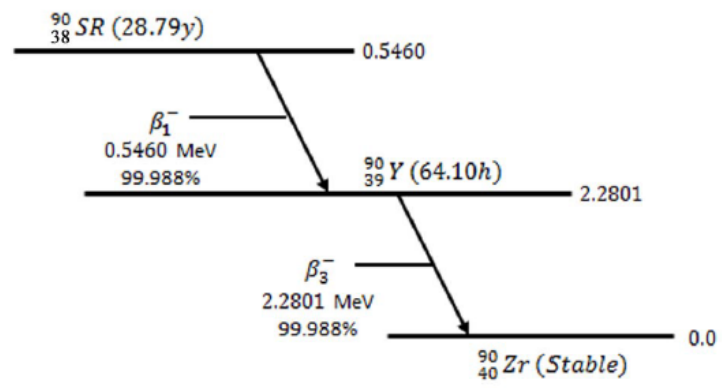


Fig. 2. Complete decay chain of Sr-90.

Pu-238 Decay Chain

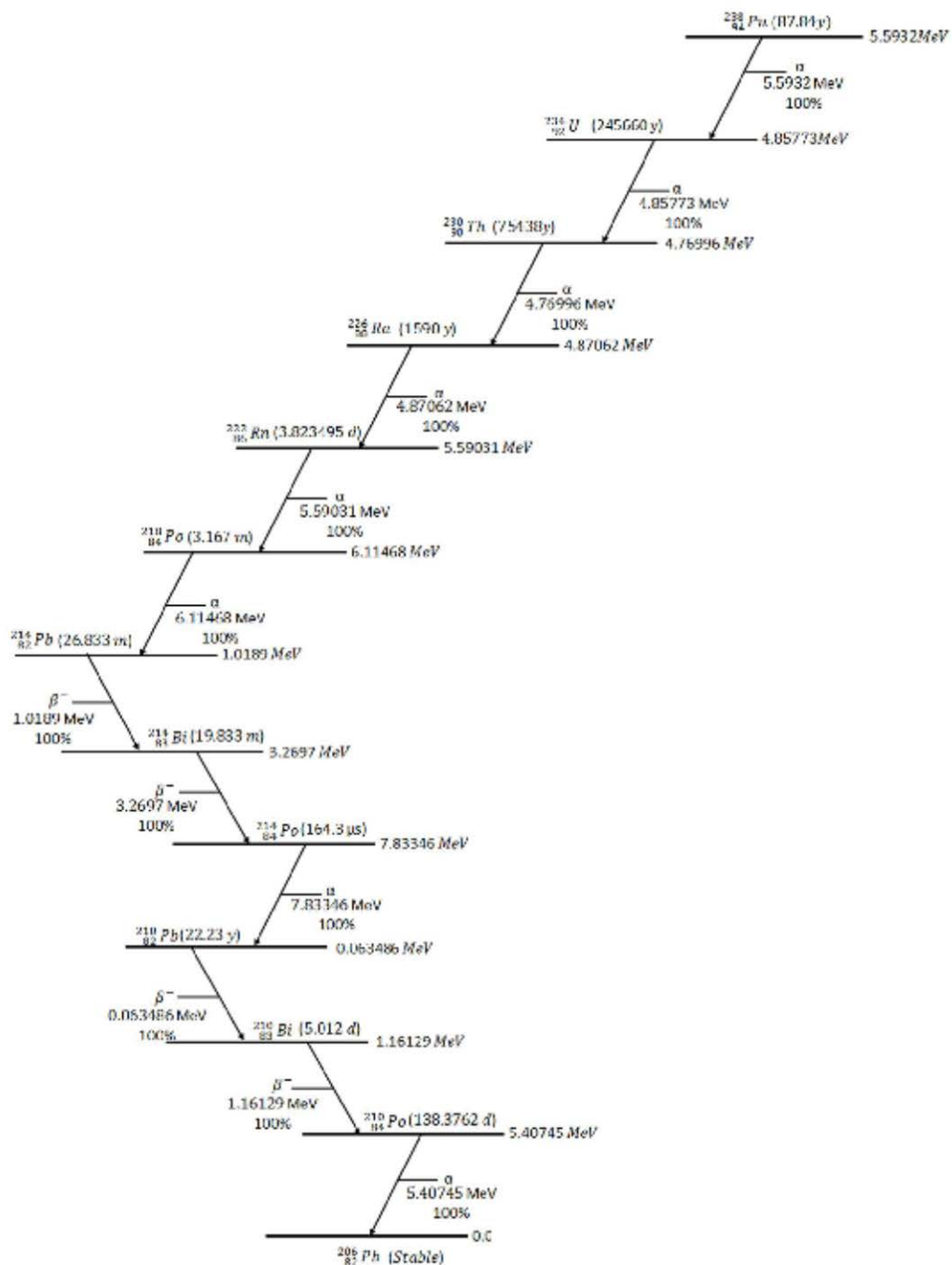


Fig. 3. Complete decay chain of Pu-238.

Another important aspect in the choice of Sr-90 over Pu-238 is because the production of Pu-238 involves a complex nuclear chain, and the quantity that could be produced in a commercial reactor is several orders of magnitude less than the quantity of Sr-90 produced, making Sr-90 a much more economical choice.

Application for Study

The application of this study is to examine the feasibility of using the Sr-90 RTG to power a home or small facility in remote locations. In 2012, the average annual electricity consumption for a home in the United States was 10,837 kWh; which is an average of 29.7 kWh per day with the daily power divided into common household appliance as described in Table 1 (U.S. Energy Information Administration 2014). This is useful information in determining the desirable power range that may be preferred for the Sr-90TiO₃ RTG.

Description	Power Required (Watts)	Hours/day of use	kWhr/day
Refrigerator (16 cubic feet)	725	24	17.4
40 gal Water Heater	5000	1.5	7.5
Clock Radio	10	24	0.24
Coffee maker	1000	0.5	0.5
Clothes Washer	425	0.29	0.12
Clothes Dryer	3500	0.29	1
Dish Washer	1800	0.5	0.9
Personal Computer	270	3	0.81
Flat Screen Television	120	3	0.36
Toaster	1000	0.03	0.03
Cabin Lighting using LEDs	100	6	0.6
Other Electronics	1000	0.23	0.23
Total kWhr/day			29.69
Total kWhr/yr			10838.59

Table 1. Energy consumption for common household appliances (U.S. Energy Information Administration 2014).

Solar power is also an effective method of powering a remote residence. Solar power works by using a bank of solar panels, and converts the sun's rays to electricity. The solar panels are then connected to a charge controller, which is a device that regulates the amount of electricity that goes to and from a battery bank, preventing the battery bank from being overcharged or drained by the solar panels. A battery bank is used to store any extra energy for when the sun is not shining. An inverter is also used to convert the direct current (DC) to alternating current (AC) which is the standard method of powering a home in the United States. The efficiency of the inverter ranges between about 50 % - 90 % depending on how much power is being used by the home. A greater efficiency occurs for the higher power usage and a lower efficiency occurs for lower power usage (Solar Facts 2014). Because of the increased energy loss that the inverter introduces to the system some have either added a generator or avoided the inverter altogether and choose to use

only DC power, which means that all appliances within the home would need to be custom built to take DC power. An illustration of an off-grid DC and AC solar power system is illustrated in Figure 4.

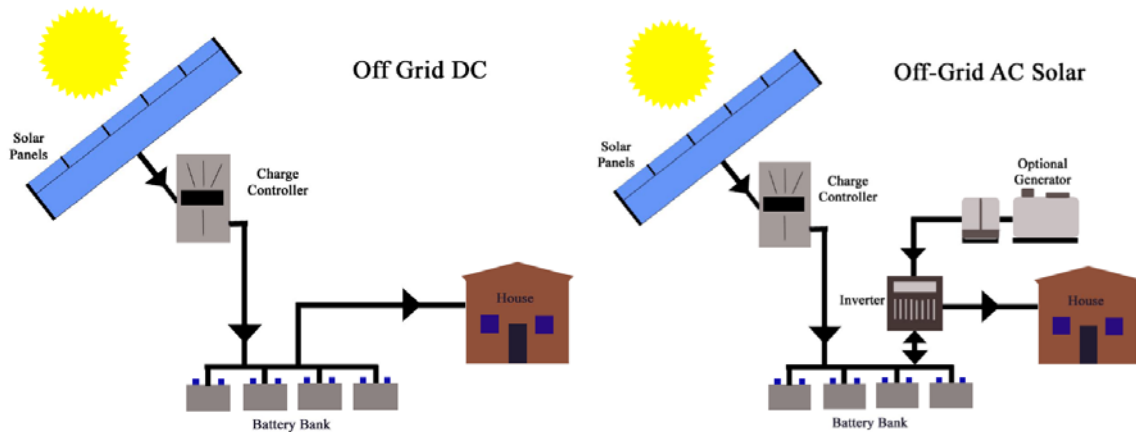


Figure 4. Off grid DC (left) and AC (right) with optional generator solar power system.

It is certainly possible to power a home in a remote location using only solar panels, but due to its inefficiencies it may not be economically viable to do so. For example, prices can range from about \$1,300 for a 36 kWh/month system to about \$18,000 for a 889 kWh/month system in purchase, installation, and startup costs plus whatever maintenance that may be required. The objective of this project sets out to evaluate the economic and technical feasibility of a possible alternative to solar powered systems.

To accomplish this objective, the design criteria for the Sr-90TiO₃ power unit would need to exceed benefits provided by the solar option, particularly for applications

where power is needed in remote locations. The first criteria to be met is that the unit would need to be of modular design, that is, it will need to be able to be connected in parallel with other units to give the customer the ability to easily meet their needs. The second criterion is that the power unit would need to be durable and have the ability to last much longer than the typical solar power system. For extremely remote locations, several years of operational lifetime would be preferable. For this reason, an operational lifetime of 30 years was chosen, and with a half-life of 28.79 years for Sr-90, this would mean that the initial power of the unit would have over double the power at the end of the operational lifetime. It was also desirable to set the amount of power at the end of the operational lifetime to be a value that would still be useful for applications such as a remote residence, which was believed to be met by designing the power unit to have at the end of its operational lifetime to be 300 Watts.

Chapter 2 - Design Criteria

Sr-90TiO₃ as a Heat Source for an RTG

The first detail to investigate while designing the RTG using Sr-90TiO₃ as a heat source was the energy density of Sr-90TiO₃. In order to find the energy density one must first find the number of radioactive atoms within the Sr-90TiO₃ and account for the energy release as each Sr-90 atom decays. The Sr-90 atom density within the Sr-90TiO₃, the use of the half-life equation, and the thermal power density produced by the Sr-90TiO₃ is found in Eqns. 4a, 4b, and 4c respectively.

$$N_{iv} = \frac{\rho A_v}{MW} = \frac{(5.11 \text{ g/cm}^3)(6.022 \times 10^{23} \text{ atoms/mol})}{185.773 \text{ g/mol}} = 1.65645 \times 10^{22} \text{ molecules/cm}^3$$

(Eqn. 4a)

Where N_{iv} = # of Sr-90 atoms per cm^3 of SrTiO₃ fuel

$$\rho = \text{density of Sr-90TiO}_3 = 5.11 \text{ g/cm}^3$$

A_v = Avogadro's Number

MW = Molecular Weight of Sr-90TiO₃

$$= (89.907738 + 47.867 + 3(15.9994)) \text{ g/mol} = 185.773 \text{ g/mol}$$

Because Sr-90 is in secular equilibrium with Y-90, it can be assumed that $T_{eq} = T_{Sr-90}$,

where T_{eq} = Equivalent half life of Sr-90 and Y-90 combined.

$$\lambda_{Sr-90} = \frac{\ln(2)}{T_{Sr-90}} = \frac{\ln(2)}{28.79 \text{ yr}} = 0.024076 \text{ yr}^{-1} \quad (\text{Eqn. 4b})$$

Or

$$\lambda_{Sr-90} = \frac{\ln(2)}{(28.79 \text{ yr}) \left(365 \frac{\text{day}}{\text{yr}}\right) \left(24 \frac{\text{hr}}{\text{day}}\right) \left(3600 \frac{\text{s}}{\text{hr}}\right)} = 7.63444 \times 10^{-10} \text{ s}^{-1}$$

Where λ_{Sr-90} = Decay constant for Sr-90

T_{Sr-90} = Half life of Sr-90

$$P_{th_ti} = N_{iv} E_{ave} \lambda_{Sr-90} \quad (\text{Eqn. 4c})$$

$$\begin{aligned} &= \left(1.65645 \times 10^{22} \text{ atoms/cm}^3\right) \left(1.145 \text{ MeV/dis}\right) \left(10^6 \text{ eV/1MeV}\right) \left(1J/6.2415 \times 10^{18} \text{ eV}\right) (7.63444 \times 10^{-10} \text{ s}^{-1}) \\ &= 2.319919 \text{ W}_{th}/\text{cm}^3 \end{aligned}$$

Where P_{th_ti} = Thermal power release per unit volume of Sr-90TiO3 fuel.

N_{iv} = # of Sr-90 atoms per cm^3

λ_{Sr-90} = The decay constant of Sr-90

E_{ave} = Average energy released for Sr-90 and Y-90 per disintegration

$$= (E_{aveSr-90} + E_{aveY-90}) = (0.201 + 0.944) \text{ MeV} = 1.145 \text{ MeV/dis}$$

Note: The values for the average energy released for Sr-90 and Y-90 was used from empirical data found and reported by ORNL (Shore et al 1971, see also Table 2).

The thermal power density can also be expressed in terms of the thermal power released per unit mass as described by Eqn. 4d.

$$P_{th_p_ti} = \frac{P_{th_ti}}{\rho} = \frac{2.31991943 \text{ W}_{th}/\text{cm}^3}{5.11 \text{ g/cm}^3} = 0.453996 \text{ W}_{th}/\text{g} \quad (\text{Eqn. 4d})$$

With the power released per unit mass one can then determine the amount of mass of the Sr-90TiO3 fuel that would be required for a minimum power output over the desired operational lifetime of the power unit. This is determined by using a form of the activity equation as is shown in Eqn. 5a. One can also calculate the thermal power released per unit volume after a given operational lifetime. This was accomplished by using the power released per unit volume initially and the activity equation. This is shown in Eqn. 5b.

$$P_{th_p_tfinal} = P_{th_p_ti} e^{-\lambda_{Sr-90} t_{op}} \quad (\text{Eqn. 5a})$$

$$= (0.453995975 \text{ } W_{th}/g) e^{-(0.024076 \text{ yr}^{-1})(30 \text{ yr})} = 0.220480 \text{ } W_{th}/g$$

Where $P_{th_p_tfinal}$ = Thermal power release per gram of Sr-90TiO3 fuel after the power device in operation for 30 yrs.

$P_{th_p_ti}$ = Thermal power release per gram of Sr-90TiO3 fuel initially.

t_{op} = Time of operation of the power device

λ_{Sr-90} = Decay constant for Sr-90

$$P_{th_tfinal} = P_{th_ti} e^{-\lambda_{Sr-90} t_{op}} \quad (\text{Eqn. 5b})$$

$$= (2.319919433 \text{ } W_{th}/cm^3) e^{-(0.024076 \text{ yr}^{-1})(30 \text{ yr})} = 1.126655 \text{ } W_{th}/cm^3$$

Where P_{th_tfinal} = Thermal power release per cubic centimeter of Sr-90TiO3 fuel after the power device in operation for 30 yrs.

P_{th_ti} = Thermal power release per cubic centimeter of Sr-90TiO3 fuel initially.

t_{op} = Time of operation of the power device

λ_{Sr-90} = Decay constant for Sr-90

The next step was to implement the decision as to how much power would be produced over how long. It was decided that the power unit would have an operational lifetime of 30 years and an electrical power output of approximately 300 W_e at the end of the operational lifetime (making the initial power output at 621 W_e). The volume of the fuel cell was used in calculating the initial and final electrical power that would be released by the device can be seen in Eqn. 5c and 5d respectively (see section “Dealing with the Heat” for discussion regarding the choice of the dimensions of the radius and height of the fuel cell).

$$P_{e_ti} = (P_{th_ti})(\varepsilon)(V) \quad (\text{Eqn. 5c})$$

$$\begin{aligned} P_{e_ti} &= \left(2.319919433 \frac{W_{th}}{cm^3}\right) (0.058483319)(4580.442089 \text{ cm}^3) \\ &= 621.458751 W_e \end{aligned}$$

$$P_{e_tf} = (P_{th_tf})(\varepsilon)(V) \quad (\text{Eqn. 5d})$$

$$P_{e_tf} = \left(1.126655324 \frac{W_{th}}{cm^3}\right) (0.058483319)(4580.442089) = 301.807813 W_e$$

Where P_{th_i} = Initial thermal power output of device

P_{e_i} = Thermal power output of device at the end of the operational life

$$V = \pi R^2 H = \pi (4.5 \text{ cm})^2 (72 \text{ cm}) = 4580.442089 \text{ cm}^3$$

Where R = Radius of fuel cell

H = Height of the fuel cell

ε = Overall efficiency of power unit = 0.058483

Note: In order to calculate the overall efficiency the thickness of the required shielding had to be determined and the decisions regarding the thermocouples had to be made. The method for determining the overall efficiency is explained in Chapter 3.

Shielding

Shielding: Dealing with Bremsstrahlung Radiation

Sr-90 is a very advantageous fuel to be used for an RTG because it, and its progeny Y-90 produces no gammas directly but the relatively high energy betas can produce X-rays via Bremsstrahlung radiation. The Bremsstrahlung radiation produced needed to be dealt with in the design of the shielding. Bremsstrahlung radiation may be produced when an electron's trajectory is altered by the pull of a positively charged nucleus as is illustrated in Fig. 5.

Bremsstrahlung Radiation (Radiative Energy Transfer Mechanism)

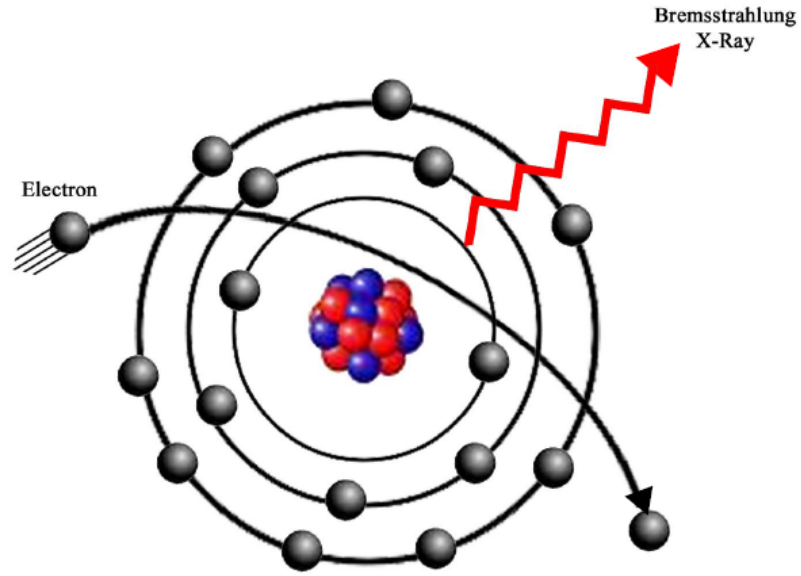


Fig. 5. Illustration of Bremsstrahlung Radiation.

An empirical method of estimating the fraction of Bremsstrahlung radiation per β^- emitted, is described in Eqn. 6a below (Johnson & Birky 2012).

$$f = 3.5 \times 10^{-4} Z E_{max} \quad (\text{Eqn. 6a})$$

Where f = fraction of the incident beta energy converted into photons

Z = Atomic number of the absorber

E_{max} = Maximum energy of the beta particle [MeV]

Although the theoretical yield was given, if there were empirical data to confirm the amount of Bremsstrahlung occurring in the Sr-90TiO3 fuel, it would be very useful. ORNL did take such data and it is described in Table 2a.

Maximum beta-particle energy			0.545 MeV	Maximum beta-particle energy			2.27 MeV
Average beta-particle energy			0.201 MeV	Average beta-particle energy			0.944 MeV
Bremsstrahlung energy group, MeV	Within ΔE energy group			Bremsstrahlung energy group, MeV	Within ΔE energy group		
	Photons per beta particle	Photons/W-sec			Photons per beta particle	Photons/W-sec	
0.020 \pm 0.01	1.009×10^{-2}	5.55×10^{10}		0.100 \pm 0.05	4.537×10^{-2}	2.50×10^{11}	
0.040 \pm 0.01	4.044×10^{-3}	2.22×10^{10}		0.200 \pm 0.05	1.782×10^{-2}	0.98×10^{11}	
0.060 \pm 0.01	2.195×10^{-3}	1.21×10^{10}		0.300 \pm 0.05	9.456×10^{-3}	5.20×10^{10}	
0.080 \pm 0.01	1.348×10^{-3}	7.41×10^9		0.400 \pm 0.05	5.665×10^{-3}	3.12×10^{10}	
0.100 \pm 0.01	8.845×10^{-4}	4.86×10^9		0.500 \pm 0.05	3.613×10^{-3}	1.99×10^{10}	
0.120 \pm 0.01	6.034×10^{-4}	3.32×10^9		0.600 \pm 0.05	2.389×10^{-3}	1.31×10^{10}	
0.140 \pm 0.01	4.217×10^{-4}	2.32×10^9		0.700 \pm 0.05	1.611×10^{-3}	0.89×10^{10}	
0.160 \pm 0.01	2.993×10^{-4}	1.65×10^9		0.800 \pm 0.05	1.098×10^{-3}	6.04×10^9	
0.180 \pm 0.01	2.141×10^{-4}	1.18×10^9		0.900 \pm 0.05	7.493×10^{-4}	4.12×10^9	
0.200 \pm 0.01	1.537×10^{-4}	8.45×10^8		1.000 \pm 0.05	5.092×10^{-4}	2.80×10^9	
0.220 \pm 0.01	1.103×10^{-4}	6.07×10^8		1.100 \pm 0.05	3.425×10^{-4}	1.88×10^9	
0.240 \pm 0.01	7.871×10^{-5}	4.33×10^8		1.200 \pm 0.05	2.264×10^{-4}	1.25×10^9	
0.260 \pm 0.01	5.571×10^{-5}	3.06×10^8		1.300 \pm 0.05	1.460×10^{-4}	8.03×10^8	
0.280 \pm 0.01	3.895×10^{-5}	2.14×10^8		1.400 \pm 0.05	9.110×10^{-5}	5.01×10^8	
0.300 \pm 0.01	2.678×10^{-5}	1.47×10^8		1.500 \pm 0.05	5.434×10^{-5}	3.00×10^8	
0.320 \pm 0.01	1.801×10^{-5}	0.99×10^8		1.600 \pm 0.05	3.050×10^{-5}	1.68×10^8	
0.340 \pm 0.01	1.179×10^{-5}	6.48×10^7		1.700 \pm 0.05	1.576×10^{-5}	8.67×10^7	
0.360 \pm 0.01	7.448×10^{-6}	4.10×10^7		1.800 \pm 0.05	7.220×10^{-6}	3.97×10^7	
0.380 \pm 0.01	4.497×10^{-6}	2.47×10^7		1.900 \pm 0.05	2.764×10^{-6}	1.52×10^7	
0.400 \pm 0.01	2.559×10^{-6}	1.41×10^7		2.000 \pm 0.05	7.850×10^{-7}	4.32×10^6	
0.420 \pm 0.01	1.345×10^{-6}	0.74×10^7		2.100 \pm 0.05	1.239×10^{-7}	6.81×10^5	
0.440 \pm 0.01	6.333×10^{-7}	3.48×10^6		2.200 \pm 0.05	3.540×10^{-9}	1.95×10^4	
0.460 \pm 0.01	2.534×10^{-7}	1.39×10^6					
0.480 \pm 0.01	7.807×10^{-8}	4.29×10^5					
0.500 \pm 0.01	1.472×10^{-8}	8.10×10^4					
0.520 \pm 0.01	7.336×10^{-10}	4.03×10^3					
0.540 \pm 0.01	0.000						
Total bremsstrahlung energy, MeV/beta particle			9.924×10^{-4}	Total bremsstrahlung energy, MeV/beta particle			2.078×10^{-2}

Table 2a. Table of average Bremsstrahlung energy produced per beta particle release for Sr-90 (left) and Y-90 (right) (Shor et al 1971).

Using the data found in Table 2, for each β^- decay of Sr-90, the total Bremsstrahlung energy per β^- was confirmed by adding the weighted average energy per photon as seen in Eqn. 6b and 6c. This is shown in Table 2b for Sr-90 and Table 2c for Y-90.

$$E_{totBrem/\beta} = Tot_{Photons/\beta} \times Tot_{weight_Eave} \quad (\text{Eqn. 6b})$$

Where $Tot_{Photons/\beta} = \text{Total \# Photons in all energy groups}$

$$Tot_{weight_Eave} = \text{sum} \left(\frac{\# \text{ photon in group } n}{Tot_{Photons/\beta}} \right) \times \text{Energy of group } n \quad (\text{Eqn. 6c})$$

Sr-90			
Energy Group #	Photons / β	Bremsstrahlung Energy (MeV)	Weighted Average Energy (MeV)
1	0.01009	0.02	0.009790993
2	0.004044	0.04	0.00784832
3	0.002195	0.06	0.00638986
4	0.001348	0.08	0.005232214
5	0.0008845	0.1	0.004291444
6	0.0006034	0.12	0.003513113
7	0.0004217	0.14	0.002864423
8	0.0002993	0.16	0.002323444
9	0.0002141	0.18	0.001869798
10	0.0001537	0.2	0.001491453
11	0.0001103	0.22	0.001177345
12	0.00007871	0.24	0.00091653
13	0.00005571	0.26	0.000702768
14	0.00003895	0.28	0.000529141
15	0.00002678	0.3	0.000389796
16	0.00001801	0.32	0.000279621
17	0.00001179	0.34	0.00019449
18	0.000007448	0.36	0.000130091
19	0.000004497	0.38	8.2911E-05
20	0.000002559	0.4	4.96633E-05
21	0.000001345	0.42	2.7408E-05
22	6.333E-07	0.44	1.35197E-05
23	2.534E-07	0.46	5.65549E-06
24	7.807E-08	0.48	1.81816E-06
25	1.472E-08	0.5	3.57095E-07
26	7.336E-10	0.52	1.85084E-08
		Total Weighted Average Energy (MeV)	
Total Photons / β	0.020611		0.050116
		Total Bremsstrahlung E (MeV)/Sr-90 β	0.001033

Table 2b. Verification of average Bremsstrahlung energy produced per beta for Sr-90.

Y-90				
Energy Group #	Photons / β	Bremsstrahlung Energy (MeV)	Weighted Average Energy (MeV)	
1	0.04537	0.1	0.050864371	
2	0.01782	0.2	0.039956054	
3	0.009456	0.3	0.031803405	
4	0.005665	0.4	0.025404158	
5	0.003613	0.5	0.020252697	
6	0.002389	0.6	0.016069868	
7	0.001611	0.7	0.012642661	
8	0.001098	0.8	0.009847755	
9	0.0007493	0.9	0.007560372	
10	0.0005092	1	0.005708648	
11	0.0003425	1.1	0.00422375	
12	0.0002264	1.2	0.003045808	
13	0.000146	1.3	0.00212785	
14	0.0000911	1.4	0.001429853	
15	0.00005434	1.5	0.00091381	
16	0.0000305	1.6	0.000547097	
17	0.00001576	1.7	0.000300365	
18	0.00000722	1.8	0.000145698	
19	0.000002764	1.9	5.88758E-05	
20	0.000000785	2	1.76013E-05	
21	1.239E-07	2.1	2.91699E-06	
22	3.54E-09	2.2	8.73114E-08	
		Total Weighted Average Energy (MeV)		
Total Photons / β	0.089198			0.232924
		Total Bremsstrahlung E (MeV)/Y-90 β		0.020776

Table 2c. Verification of average Bremsstrahlung energy produced per beta for Y-90.

As is displayed in Table 2b, it was found that 0.001033 MeV of energy is released from Bremsstrahlung X-Rays for every β^- decay of Sr-90. It was also found that 0.020611 photons were released per β^- decay of Sr-90. As is displayed in Table 2c, it was found that 0.020776 MeV of energy is released from Bremsstrahlung X-Rays for

every β^- decay of Y-90. It was also found that 0.089198 photons were released per β^- decay of Y-90.

In order to account for the Bremsstrahlung radiation there were multiple options: The first option was to put a low Z material immediately outside the fuel element to stop the β^- s while minimizing the Bremsstrahlung. This low Z material would need to have good heat conducting properties, a high melting point, and have adequate strength to be a viable option. With an atomic number of 13, Aluminum (Al) appeared to be an ideal candidate to be considered. With an atomic number of 23 and good heat conducting and material properties, Iron (Fe) was also considered. The second option was to add an additional amount of a very dense material such as Lead (Pb) or depleted Uranium (U) to shield both the beta particles and the Bremsstrahlung that occurs in increased amounts as a result of the high Z material. The third option was a combination of the first two options.

Shielding: β^- Particle Range

With Al, Fe, Pb, and U being considered as a shielding option to minimize Bremsstrahlung radiation, and understanding that there will be some self shielding within the Sr-90TiO₃ fuel cell, the range of the maximum energy beta particle from Sr-90 and its progeny Y-90, which was 2.27 MeV, had to be considered. The range of a 2.27 MeV beta particle through Al, Fe, Pb, U, and Sr-90TiO₃ can be described by Eqn. 7 (Cember 2009)

$$R = 0.542E - 0.133 \quad \text{for } E \geq 0.8 \text{ MeV} \quad (\text{Eqn. 7})$$

$$\text{Where } R = \text{Range in } \frac{g}{cm^2} = 0.542(2.27) - 0.133 = 1.09734 \frac{g}{cm^2}$$

E = Maximum beta energy in MeV

Using Eqn. 7 one need only divide R by the density of the material being considered.

Realizing that the density of Al, Fe, Pb, and Sr-90TiO3 are $2.7 \frac{g}{cm^3}$, $7.874 \frac{g}{cm^3}$, $11.34 \frac{g}{cm^3}$, $19.1 \frac{g}{cm^3}$, and $5.11 \frac{g}{cm^3}$ respectively and the maximum beta energy from Sr-90 and its

progeny is 2.27 MeV, the maximum range of a beta particle in Al, Fe, Pb, U, and Sr-90TiO3 was found to be 0.41 cm, 0.14 cm, 0.097cm, 0.057 cm, and 0.215 cm respectively. With air at standard temperature and pressure having a density of $0.001275 \frac{g}{cm^3}$, the range of the 2.27 MeV β^- particle in air was found to be 860.4 cm or 28.22 ft (if

the situation of the shielding being removed should occur). However, 0.5 cm of any of the metals cited will eliminate all beta radiation.

With air at standard temperature and pressure having a density of $0.001275 \frac{g}{cm^3}$, the range of the 2.27 MeV β^- particle in air was found to be 860.4 cm or 28.22 ft (if the situation of the shielding being removed should occur). However, 0.5 cm of any of the metals cited will eliminate all beta radiation.

However, 0.5 cm of any of the metals cited will eliminate all beta radiation.

Shielding: Calculating Buildup Factor

When using a material to shield photons of a great enough energy, there is a high likelihood of multiple collisions that the photon makes before slowing down completely and dissipating its energy into the material. When the shielding material is thick enough much more collisions occur and enough energy is transferred to the material, which may become radioactive. This is known as radiation buildup and is illustrated in Figure 6.

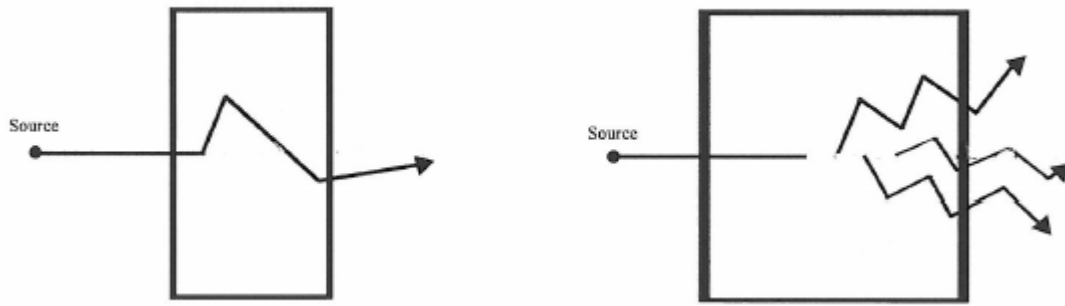


Fig. 6. Illustration of radiation buildup avoided (left) and occurring in material (right).

However, if the energy of the photon is low enough, when the photon strikes an orbiting electron all of the energy from the incident photon is transferred to the orbiting electron and there is no radiation buildup, which is what occurs in the photo-electric effect. For Sr-90 and its progeny Y-90, the average energy of the photons released are 50 keV and 200 keV respectively. As can be seen in Fig. 7 the photon interactions for both the Sr-90 and Y-90 Bremsstrahlung photons will be dominated by the photo-electric effect and therefore it is not necessary to account for radiation buildup in the shielding calculations if a material of high density such as Pb or U is used. The photo-electric effect, Compton scattering, and pair production are represented by μ_{pe} , μ_{cs} , and μ_{pp} respectively.

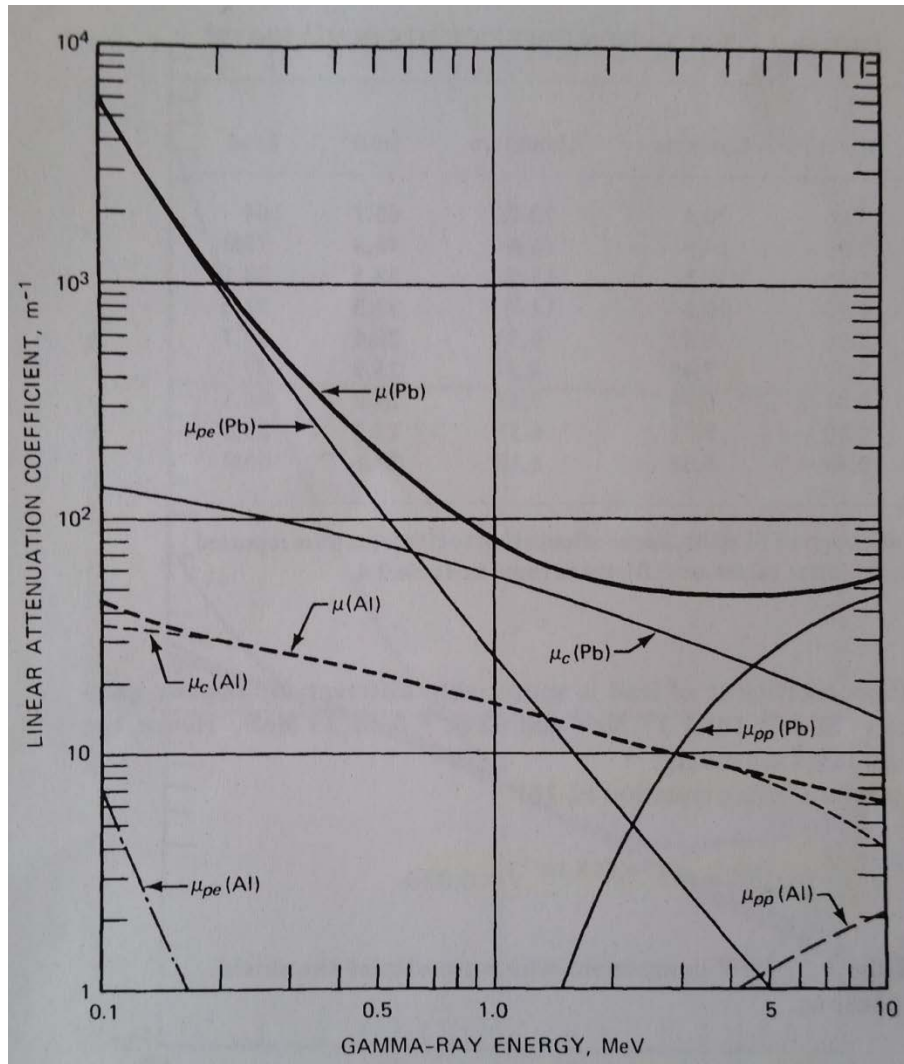


Fig. 7. Linear attenuation coefficient for Pb vs. photon energy (Glasstone & Sesonske 2010).

Shielding: Calculating Thickness

When calculating the necessary thickness to shield all the photons produced by the Bremsstrahlung radiation it was decided to take the second option; that is, to use a more dense material - depleted Uranium (U) even though it has a tendency to produce a higher amount of Bremsstrahlung radiation. The increased amount of Bremsstrahlung produced due to the U is accounted for in the increased shielding effectiveness.

In order to be more accurate when calculating the necessary shielding the cylindrical geometry was accounted for. This was accomplished by first solving for the flux (or fluence rate) of the gamma radiation exiting the fuel cell as and passing through the shielding material. This is described in Eqns. 8a, and 8b.

$$\emptyset_{cyl}(z, t) = \frac{S_V R^2}{4(a+z)} [F(\theta_1, \mu t + \mu_V d) + F(\theta_2, \mu t + \mu_V d)] \quad (\text{Eqn. 8a})$$

$$\text{Where } F(\theta_1, \mu t + \mu_V d) = \int_0^{\theta_1} e^{-\mu t \sec \theta} d\theta \quad (\text{Eqn. 8b})$$

There is no rigorous solution to Eqn. 8b. In fact it is known as the Sievert Integral and must be solved iteratively. To be conservative as well and to simplify Eqn. 8a, it was assumed that $\theta_1 = \theta_2$, which is the point at which the highest dose would be received by an individual standing near the power unit along a perpendicular center line. This is illustrated in Fig. 8. The simplified equation for \emptyset_{cyl} is shown below the illustration and is Eqn. 8c (Jaeger et al 1968). Eqn. 8c was used to solved for \emptyset_{cyl} due to the Bremsstrahlung radiation caused by both Sr-90 and Y-90. The activity of gammas released per unit volume from Sr-90 and Y-90 are given in Eqns. 8d and 8e respectively.

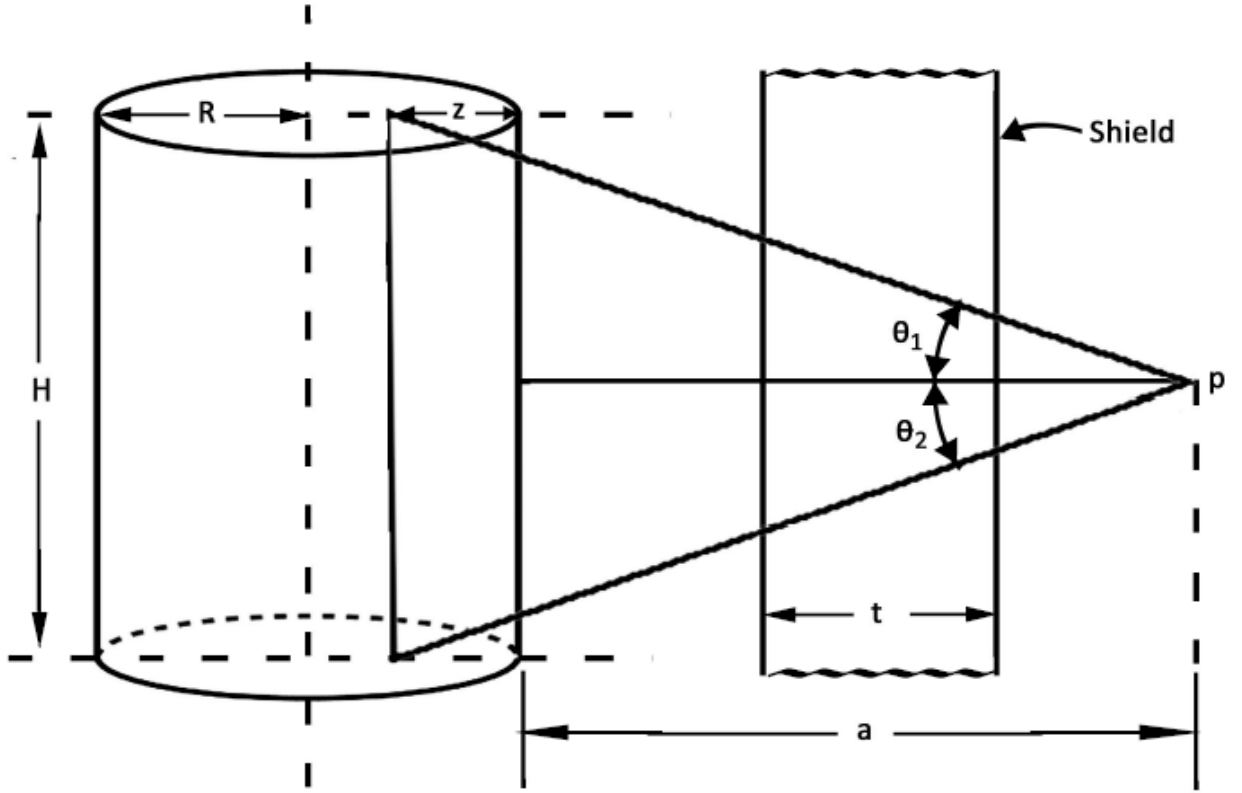


Fig. 8. Illustration of cylindrical fuel cell with a shield and variable labels.

$$\phi_{cyl} = \frac{BS_V R^2}{2(a+z)} F(\theta, b_2) \quad (\text{Eqn. 8c})$$

Or

$$\phi_{cyl_Sr-90} = \frac{BS_{V_{Sr-90}} R^2}{2(a+z)} F(\theta, b_2) \quad \text{for flux due to Sr-90}$$

Or

$$\phi_{cyl_Y-90} = \frac{BS_{V_{Y-90}} R^2}{2(a+z)} F(\theta, b_2) \quad \text{for flux due to Y-90}$$

Where

$$S_{V_{Sr-90}} = \frac{N\lambda_{Sr-90}Y_{Sr-90}}{V} \quad (\text{Eqn. 8d})$$

$$S_{V_{Sr-90}} = \frac{(7.58729 \times 10^{25} \text{ Sr-90 atoms}) \left(7.63444 \times 10^{-10} \frac{1}{s}\right) (0.020610779 \text{ photons}/\beta)}{4580.442089 \text{ cm}^3}$$

$$= 2.60646 \times 10^{11} \text{ photons}/\text{cm}^3 \text{ s}$$

$$S_{V_{Y-90}} = \frac{N\lambda_{Sr-90}Y_{Y-90}}{V} \quad (\text{Eqn. 8e})$$

$$S_{V_{Y-90}} = \frac{(7.58729 \times 10^{25} \text{ Sr-90 atoms}) \left(7.63444 \times 10^{-10} \frac{1}{s}\right) (0.089197996 \text{ photons}/\beta)}{4580.442089 \text{ cm}^3}$$

$$= 1.12801 \times 10^{12} \text{ photons}/\text{cm}^3 \text{ s}$$

B = Buildup factor (equals 1 because no buildup in this case as discussed earlier)

R = radius of fuel cell

a = distance from beginning of self shielding to point of dose measurement

$$b_2 = \mu_f z + b_{1_current} \quad (\text{Eqn. 8f})$$

$$b_{1_current} = \sum_{i=1}^n b_{1i} \quad (\text{Eqn. 8g})$$

$$b_1 = \mu_t t = \text{Thickness attenuation length} = \text{mean free path in thickness} \quad (\text{Eqn. 8h})$$

$S_{V_{Y-90}}$ = activity of gammas per unit volume in the fuel cell due to Y-90

$S_{V_{Sr-90}}$ = activity of gammas per unit volume in the fuel cell due to Sr-90

z = distance of self-shielding within fuel cell

$F(\theta, b_2)$ = Value based on solution to Sievert integral (explained below)

$$N = N_{iv} V = \left(1.65645 \times 10^{22} \text{ Sr-90 atoms}/\text{cm}^3\right) (4580.442089 \text{ cm}^3)$$

$$= 6.16142 \times 10^{25} \text{Sr} - 90 \text{ atoms within fuel cell}$$

$$V = \text{Volume of the fuel cell} = 4580.442089 \text{ cm}^3$$

$$\theta_i = \tan^{-1} \left(\frac{H/2}{z + t_1 + t_2 + \dots + t_n} \right) \quad (\text{Eqn. 8i})$$

Where H = Height of power unit

To solve for $F(\theta, b_2)$ the first step is to calculate $\frac{a}{R}$. If $\frac{a}{R} \leq 10$, use the following

list of instructions:

Step 1) Determine μ_s , for the source, or μ_t for the given thickness

$$\left(\mu_s = 0.74606 \frac{1}{\text{cm}} \right).$$

Step 2) Obtain m by using Fig 9.a, using $\frac{a}{R}$ and $\mu_s(R + a)$.

Step 3) Solve Eqn. 8h for $b_1 = \mu_t t$.

Step 4) Solve Eqn. 8g for $b_{1_current} = \sum_{i=1}^n b_{1i}$, which accounts for all applicable thicknesses.

Step 5) Obtain $\frac{\mu_s z}{m}$ by using Fig. 9b, using $\frac{a}{R}$ and $b_{1_current}$.

Step 6) Solve for z by multiplying $\frac{\mu_s z}{m}$ found in Step 4 by $\frac{m}{\mu_s}$ obtained in Step 1 and 2.

Step 7) Solve Eqn. 8f for $b_2 = \mu_s z + b_{1_current}$ using values found in Steps 1, 4, and 6.

Step 8) Solve Eqn. 8i for $\theta_i = \tan^{-1} \left(\frac{H/2}{z + t_1 + t_2 + \dots + t_n} \right)$ for the given thickness.

Step 9) Obtain $F(\theta, b_2)$ from Fig. 10a – 10d using b_2 and θ_i found in Steps 7 and 8.

Step 10) Solve Eqn. 8c for \emptyset_{cyl} using $F(\theta, b_2)$ obtained in step 9 and other values previously determined.

Step 11) Obtain the flux to dose multiplier from Fig. 11 using \emptyset_{cyl} and the Energy of the Bremsstrahlung photons (50 keV for Sr-90 which leads to $8,000,000 \frac{\gamma s/cm^2 s}{1^R/hr}$ at 1 m away, and 200 keV for Y-90 which leads to $3,000,000 \frac{\gamma s/cm^2 s}{1^R/hr}$ at 1 m away).

Step 12) Solve Eqn. 8j to convert the flux to equivalent dose rate.

$$H[\frac{Rem}{hr}] = (\emptyset_{cyl} \gamma s/cm^2 s) \left(\frac{1^R/hr}{3,000,000 \gamma s/cm^2 s} \right) \left(\frac{0.869 Rad}{R} \right) \quad (\text{Eqn. 8j})$$

$$\text{Where Absorbed Dose (D)} = \dot{X} \left(\frac{0.869 Rad}{R} \right)$$

$$\text{Equivalent Dose (H)} = D Q_T [Rem]$$

Where Q_T = Quality Factor = 1 for gammas

Note: The μ_s for Sr-90TiO3 could not be found so the mass attenuation coefficient for Fe was used, which was then multiplied by the density of Sr-90TiO3 to obtain the value for μ_s (Radiological Health Handbook 1970).

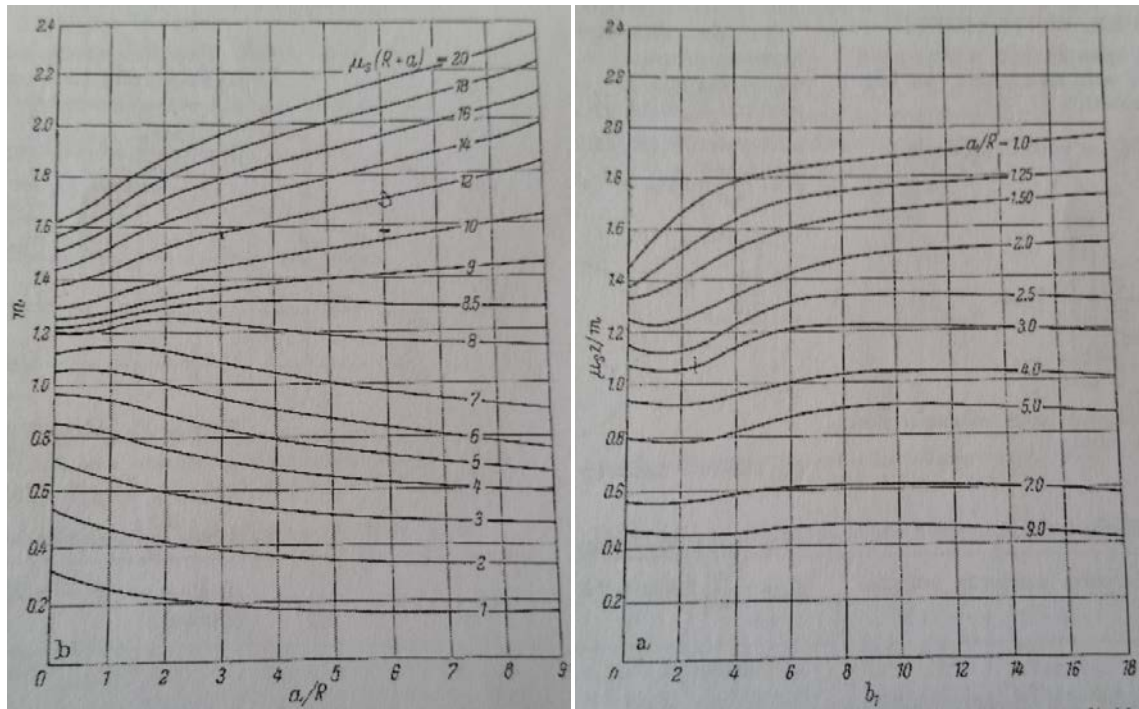


Fig. 9a & 9b. Parameter m vs. a/R (left). Function of cylinder self absorption exponent divided by $m \frac{\mu_{sz}}{m}$ (right) (Jaeger et al 1968).

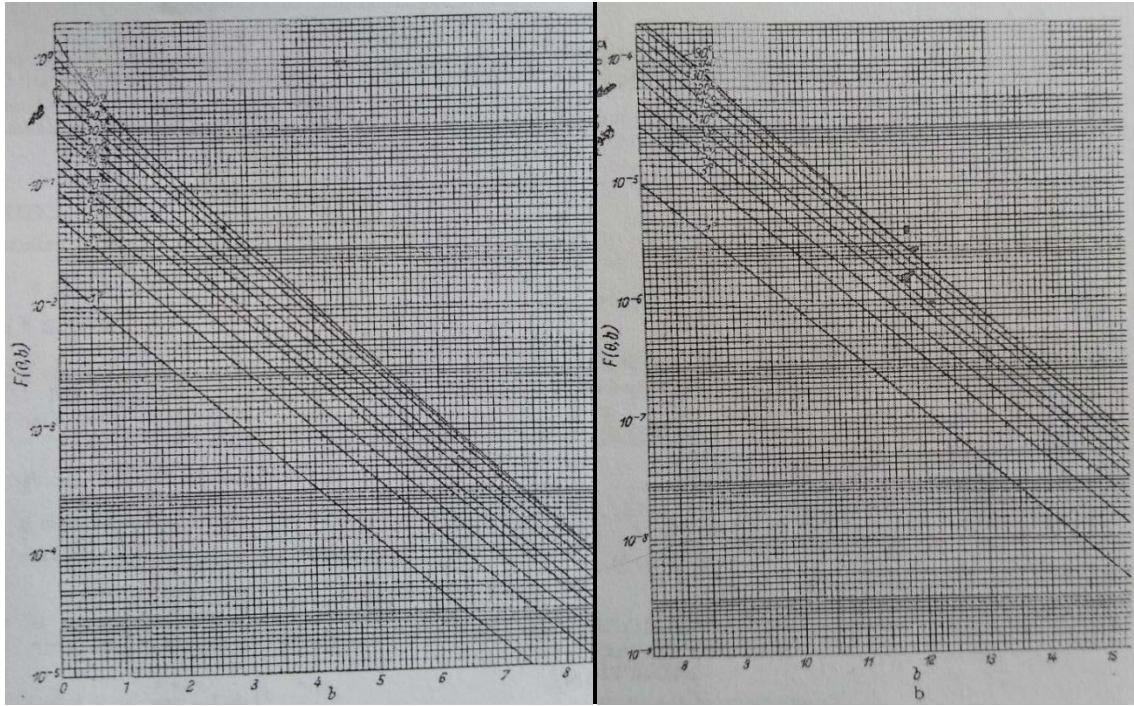


Fig. 10a and Fig. 10b $F(\theta, b_2)$ vs b_2 for $b_2 = 0$ to 8 (left) and $b_2 = 8$ to 15 (right) (Jaeger et al 1968).

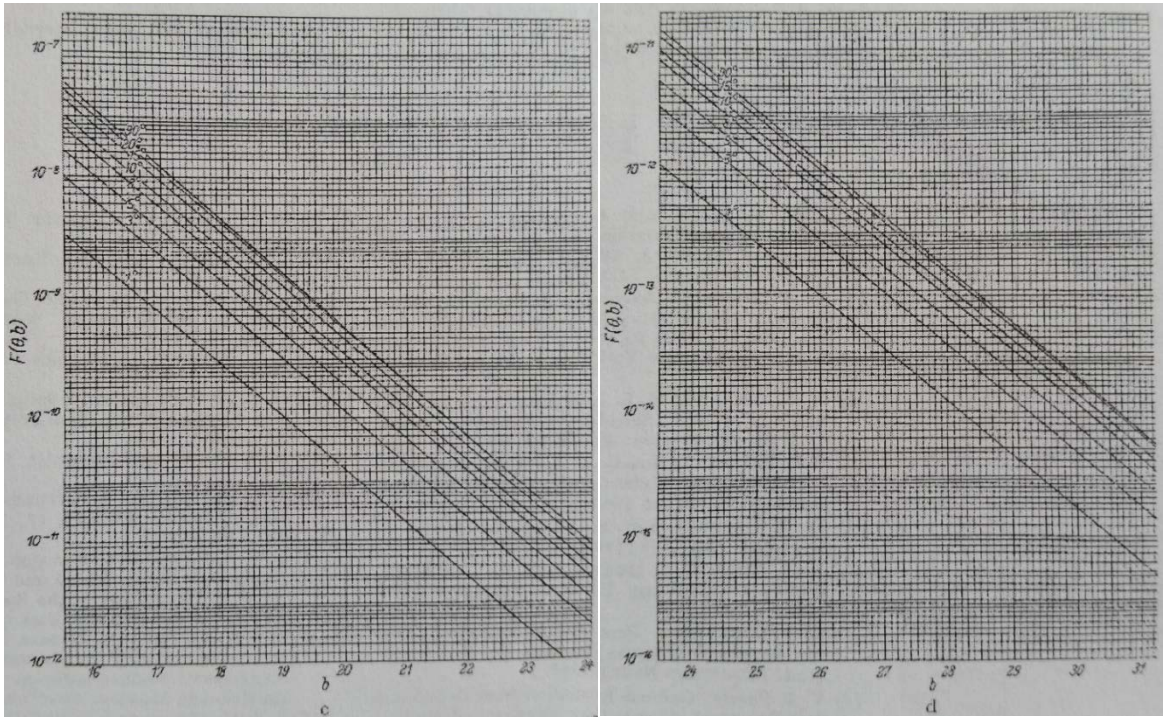


Fig. 10c and Fig. 10d $F(\theta, b_2)$ vs b_2 for $b_2 = 16$ to 24 (left) and $b_2 = 24$ to 31 (right) (Jaeger et al 1968).

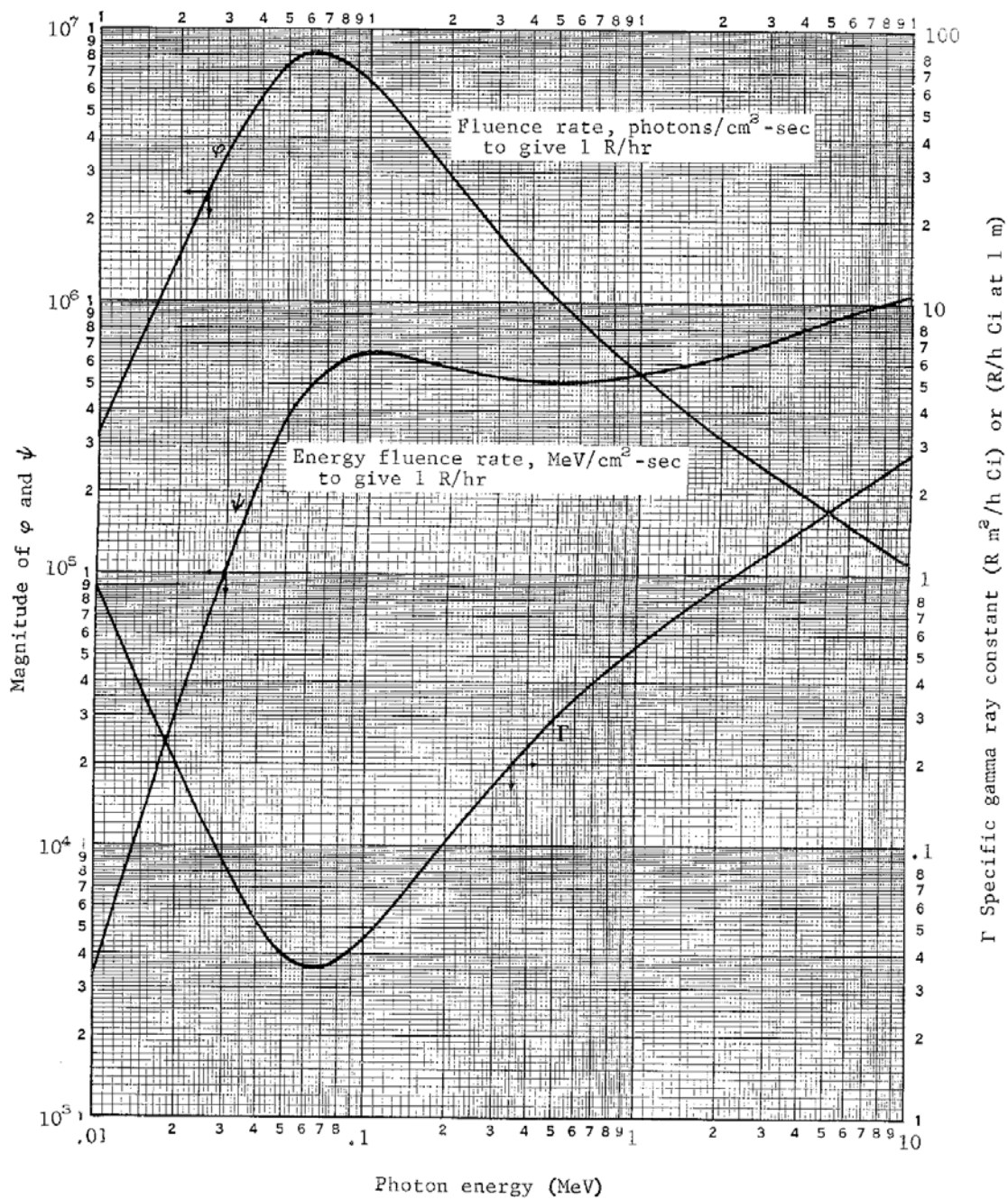


Fig. 11. Specific gamma ray constants $\left[\frac{R\text{m}^2}{\text{hrCi}}\right]$ or $\left[R \text{ at } \frac{1\text{m}}{\text{hrCi}}\right]$ and conversion factors (Radiological Health Handbook, 1970)

If $\frac{a}{R} \geq 10$, obtain $\mu_s z$ from Fig. 12 and solve for z . Then solve for the dose by following steps 6 through 12 of the previous list of instructions.

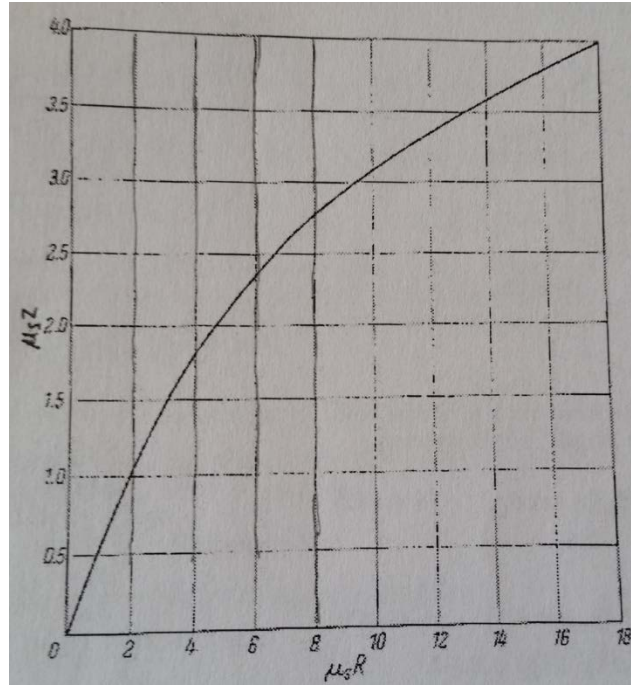


Fig. 12. Fuel cylinder self-absorption exponent $\mu_s z$ as a function of $\mu_s R$ for $\frac{a}{R} \geq 10$ (Jaeger et al 1968).

Using the 12 step process previously described, the dose rate reduced by the depleted U shielding was evaluated by investigating various shielding thicknesses before deciding on the shield thickness of 0.9 cm of depleted U to produce a dose rate of $4.159 \times 10^{-6} \text{ Rem/hr}$ at the outside surface of the U shielding, caused by Y-90, which is about 2 orders of magnitude smaller than background radiation. After the remaining consecutive annular layers are added it comes to $0.44 \times 10^{-6} \text{ Rem/hr}$ at the prime surface (the base of the outer layer) of the power unit. This may seem excessive, but this

value was decided upon as a selling point to the public, who often fear anything to do with nuclear energy. Table 3 shows the thicknesses of depleted U investigated and corresponding dose rates for the power unit as well as the corresponding values obtained using the figures mentioned in the 12 step process previously mentioned. The dose rate caused by Sr-90 was also investigated and was found to be negligible (10^{-65} Rem/hr) even at the smallest thickness.

Y - 90 Dose at Surface of Shielding				
Thickness of Shield (cm)	m	Value used to solve for Z ((μ_s z)/m)	F(θ, b_2)	Dose (Rem/hr)
0.5	0.85	2.15	9.5E-08	0.084954
0.6	0.9	2.15	8.5E-09	0.007079
0.7	0.91	2.15	7.5E-10	0.000609
0.8	0.91	2.2	6.5E-11	5.08E-05
0.9	0.92	2.21	5.5E-12	4.159E-06
1	0.93	2.22	4.5E-13	3.296E-07
1.1	0.94	2.3	4.5E-14	3.136E-08
1.2	0.95	2.3	5E-15	3.391E-09

Table 3. Thicknesses, Figure values, and corresponding dose rates investigated.

Shielding: Choice of Shielding Material

It was also desirable to calculate the mass of each layer to assist in determining the overall mass of the power unit as well as the amount of Sr-90TiO₃ and depleted U needed for each power unit. This was accomplished by using Eqns. 9a, which shows the calculation used to determine the mass of the fuel cell and 9b, which shows the calculation used to determine the mass of the depleted U used for shielding.

$$m_{fuel} = \pi R^2 H \rho \quad (\text{Eqn. 9a})$$

$$= \pi (4.5 \text{ cm})^2 (72 \text{ cm}) \left(5.11 \frac{\text{g}}{\text{cm}^3} \right) = 23.406 \text{ kg}$$

$$m_{n_layer} = \pi [(R + 2a_n)^2 (H + 2a_n) - (R + 2a_{n-1})^2 (H + 2a_{n-1})] \rho_n \quad (\text{Eqn. 9b})$$

$$\begin{aligned} &= \pi [(4.5 \text{ cm} + 1.65 \text{ cm})^2 (72 \text{ cm} + 2(1.65 \text{ cm})) \\ &\quad - (4.5 \text{ cm} + 0.75 \text{ cm})^2 (72 \text{ cm} + 2(0.75 \text{ cm}))] \left(19.1 \frac{\text{g}}{\text{cm}^3} \right) \\ &= 49.335 \text{ kg} \end{aligned}$$

Where R = radius of fuel cell

H = Height of fuel cell

ρ = Density of the Sr-90TiO3 fuel

R_n = Radius of current layer

R_{n-1} = Radius of previous layer

H_n = Total height of current power unit layer

H_{n-1} = Total height of previous power unit layer

ρ_n = Density of material in current layer

a_n = Thickness of all layers after fuel cell up to current layer

a_{n-1} = Thickness of all layers after fuel cell up to current layer - 1

Other possible shielding materials (U, Pb, and Fe) were looked at and it was found that depleted U was the material that required the thinnest layer of material as well as the smallest amount of mass. The material with the greatest density and highest

atomic weight creates the most opportunities for the photons to interact and therefore for the radiation to be shielded within a given thickness. This is shown in Table 4.

Material	Dose [Rem/hr] at Outside Surface of Shielding	Shielding Thickness [cm]	μ_{Y-90} [1/cm]	Shielding Volume [cm³]	Shielding Mass [g]
Uranium (U)	4.159E-06	0.9	24.448	2582.987635	49335.06382
Lead (Pb)	4.145E-06	1.483	14.5152	4414.157429	50056.54524
Iron (Fe)	4.175E-06	2.38	8.9344	7756.284524	54138.86598

Table 4. Shielding thicknesses and mass of U, Pb, and Fe.

Dealing with the Heat

Dealing with the Heat of the Fuel Cell

With the shielding material and thickness determined the next step was to use the appropriate heat transfer equations to describe how the heat was dealt with in the device. The first section to characterize was the transfer of heat from the center of the fuel cell to the outer edge of the cell which comes in contact with the shielding and is described by Eqn. 10a. The heat transfer coefficient of the Sr-90TiO3 fuel cell was determined by Oak Ridge during their material properties testing and is described by Eqn. 10b (Shore et al 1971, Glasstone & Sesonske 2010).

$$T_0 = T_1 + \frac{Qa_0^2}{4K_0} \quad (\text{Eqn. 10a})$$

$$T_0 = 1104.907 \text{ K} + \frac{(2.3199 \text{ W/cm}^3)(4.5 \text{ cm})^2}{4(0.028602973 \text{ W/cm K})} = 1515.515 \text{ K}$$

Where T_0 = Temperature of the center of the fuel cell [K]

T_1 = Temperature of surface of fuel cell (discussed in next section) [K]

$P_{th_ti} = Q$ = Heat generated per unit time and volume in the fuel cell
 $\left[\text{W/cm}^3 \right]$

$$= 2.319919 \text{ W}_{th}/\text{cm}^3 \quad (\text{Eqn. 4c})$$

$a_0 = R$ = Radius of fuel cell = 4.5 cm

K_0 = Heat conductivity of the fuel cell material = 0.028603 W/cm K

$$K_0 = \frac{1}{55.76+0.0673T} \left(\frac{\text{cal}}{\text{cm s}} \right) \left(\frac{4.184 \text{ J}}{1 \text{ cal}} \right) = 0.028603 \text{ W/cm K} \quad (\text{Eqn. 10b})$$

Where T = assumed average temperature of fuel cell = 1345 K

While performing the analysis it was found to be very beneficial to keep the radius of the fuel relatively small, between 4 and 6 cm for two reasons. First, as the calculations were performed to simulate fuel cell with radii between 7 and 12 cm, it was found that there became a large temperature gradient between the outer edge of the fuel cell and the center. The temperature gradient was large enough to be destructive and exceeded the melting points of the some of the materials that would be used within the power device (melting points of materials used are found in Chapter 3). The second reason for the benefit of the fuel cell having a relatively smaller radius was to increase the surface in order to maximize the amount of thermocouples that were able to be used (also explained further in Chapter 3).

Dealing with the Heat of the Intermediate Layers of the Power Unit

The next heat transfer section that was evaluated deals with the layers between the outer edge of the fuel cell and all of the other layers where conduction is the mode of heat transfer and is described by Eqn. 11. Because there were several components within several intermediate layers, the numerical values for each intermediate layer are not shown here but can be seen in a later section.

$$T_1 = T_2 + \frac{Qa_0^2}{4K_1} \ln\left(\frac{b_1}{a_1}\right) \quad (\text{Eqn. 11})$$

Where T_1 = Temperature of the inner surface of the layer being evaluated

T_2 = Temperature of the outer surface of the layer being evaluated

$Q = P_{th_ti}$ = Heat generated per unit time and volume in the fuel cell
 $\left[W/cm^3\right]$

$$= 2.319919 \text{ } W_{th}/cm^3 \quad (\text{Eqn. 4c})$$

K_1 = Heat conductivity of the layer being evaluated

a_0 = Radius of fuel cell = 4.5 cm

b_1 = Radius of outer wall of the layer being evaluated

a_1 = Radius of inner wall of the layer being evaluated

Dealing with the Heat through Proper Thermocouple Design

There were several materials that have been used in the thermocouple portion of RTGs including the following: bismuth telluride (BiTe), lead telluride (PbTe), tellurides

of antimony, germanium, silver (TAGS), lead tin telluride (PbSnTe), and silicon germanium (SiGe). All materials mentioned have been shown to be reliable and robust materials for RTGs. For all the telluride materials the maximum hot junction temperature is 550°C , but for SiGe the maximum hot junction temperature is 1000°C (Lange & Carroll 2008). For this reason, in the design of the RTG, it was assumed that SiGe will be used as the thermoelectric material which will be operating at approximately 795°C . It was also found that the maximum energy efficiency of the SiGe material is 10% (Shor et al 1971). However to match given results from the type of thermocouple that will be used in this application, the thermocouples used were assumed to have an operating efficiency of 7.5%.

When a thermoelectric material is placed between a heat sink and a heat source the temperature gradient across the thermoelectric material (also known as a thermocouple) creates a Seebeck voltage (Lange & Carroll 2008). If the Seebeck voltage is connected in series with a load a small current is produced as is illustrated in Fig. 13.

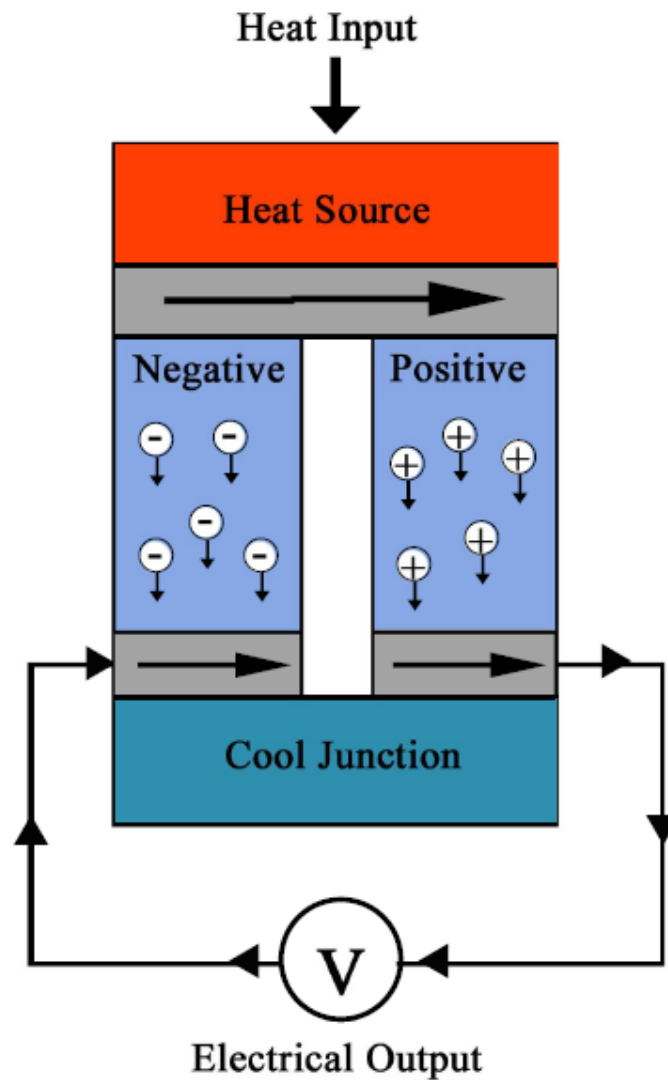


Fig. 13. Illustration of a functioning thermocouple.

If several thermocouples are placed in series within the temperature gradient, a current large enough to be useful can be produced. In some cases thermocouples are connected in both a series and parallel configuration. The series configuration is for the reason stated above and the parallel configuration is to enhance the reliability of the RTG by minimizing the effect on the total power if a single thermocouple fails. An exploded

view of the thermocouple that was used in the design of the power unit can be seen in Fig. 14.

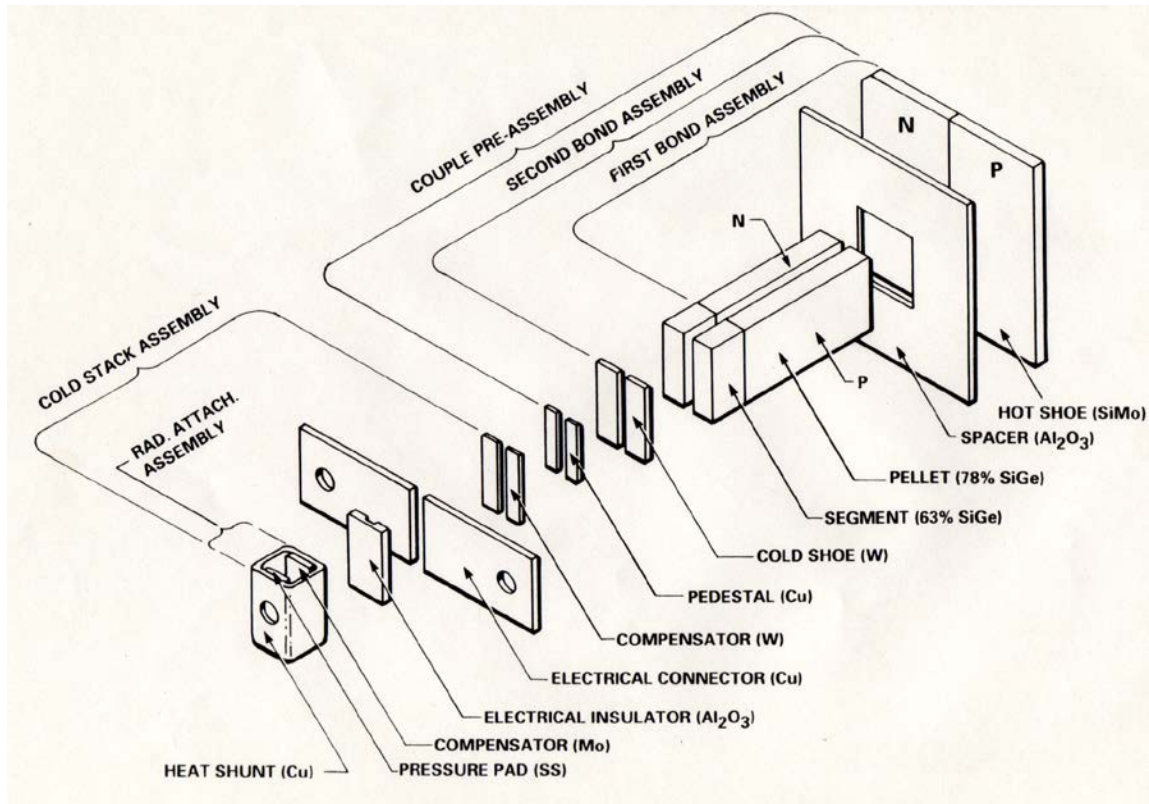


Figure 14. Exploded view of the thermocouple used in RTG design (Bennet et al 2006).

Some of the intermediate layers contained components of the array of thermocouples used to convert the heat produced into electricity. For the intermediate layers that contained the components of the thermocouple the conductivity of the layer depended on both the conductivity of the component as well as the conductivity of the surrounding insulation (woven quartz, $k = 0.0138 \text{ W/cm K}$). In some cases there were multiple component within the same layer, all cases are described by Eqn. 12.

$$k_{eff} = k_{comp} \frac{SA_{comp}}{SA_{tot}} + k_{quartz} \frac{SA_{quartz}}{SA_{tot}} \quad (\text{Eqn. 12})$$

$$= \left(0.083 \frac{W}{cm \ K} \right) \left(\frac{2 \text{ ea. } x .274 \text{ cm } x .65 \text{ cm } x (450 + 18)}{3252.473281 \text{ cm}^2} \right) \\ + \left(0.0138 \frac{W}{cm \ K} \right) \left[1 - \frac{2 \text{ ea. } x .274 \text{ cm } x .65 \text{ cm } x (450 + 18)}{3252.473281 \text{ cm}^2} \right] \\ = 0.017347 \frac{W}{cm \ K}$$

$$SA_{tot} = 2a(R + a)[H + R + 2a]$$

$$= 2\pi(1.94 \text{ cm})(4.5 \text{ cm} + 1.94 \text{ cm})[72 \text{ cm} + 4.5 \text{ cm} + 2(1.94 \text{ cm})] \\ = 3252.47281 \text{ cm}^2$$

Where k_{eff} = Effective conductivity of layer of Pellet, Segment, and Blanket [W/cm K]

k_{comp} = Conductivity of the pellet and segment [W/cm K]

k_{quartz} = Conductivity of the quartz blanket [W/cm K]

SA_{comp} = Surface area of the pellet and segment [cm^2]

SA_{tot} = Total surface area of given layer [cm^2]

Because there were several layers of various components the numerical values to solve for the effective conductivity of each layer was not given in equation form but is presented in Table 5.

Material Description (With Woven Quartz Blanket)	Material	Thick ness [cm]	Piece k [W/cm K]	Surface Area Description (All Multiplied by # of Thermocouples)	k eff [W/cm K]
Hot Shoe	SiMo	0.19	1.34	(2.29 x 2.29) cm (2.29 x 2.29) - (2 x (.274 x .65))	1.0693
Spacer	Al2O3	0.1	0.3	cm Aprox.	0.2188
Pellet and Segment	SiGe	4	0.083	(.274 x .65) cm 2 ea.	0.0173
Cold Shoe	W	0.08	1.73	(.274 x .65) cm 2 ea. Aprox	0.0631
Pedestal	Cu	0.03	4.01	(.5*.274 x .65) cm 2 ea. Aprox.	0.0707
Compensator Electrical	W	0.03	1.73	(.75*.274 x .65) cm 2 ea. Aprox. (.65 x 2.29 - .65 x .2 -	0.0321
Connector	Cu	0.09	4.01	2*pi()*(.1^2) cm Aprox.	0.4249
Electrical Insulator	Al2O3	0.09	0.3	(.55 x .65) cm Aprox.	0.0224
Heat Shunt Inside	Cu	0.05	4.01	(.47 x .65) cm Aprox.	0.1087
Heat Shunt - Compensator	Mo	0.05	1.38	(.35 x .65) cm Aprox.	0.0378
Heat Shunt Legs	Cu	0.27	4.01	(.05 x .65) cm Aprox. 2 ea.	0.0338
Heat Shunt - Pressure Pad	SS	0.05	0.155	(.35 x .65) cm Aprox.	0.0162
Heat Shunt Outside	Cu	0.05	4.01	(.47 x .65) cm Aprox.	0.1043

Table 5. Thermocouple components with effective conductivity coefficient.

Dealing with the Heat at the Outer Layer of the Power Unit

The next heat transfer section that was covered was the layer that was the outermost portion of the power unit, where both conduction and convection are applicable modes of heat transfer and is described by Eqn. 13.

$$T_s = T_m + \frac{Qa_0^2}{2} \left[\frac{1}{K_n} \ln \left(\frac{b_n}{a_n} \right) + \frac{1}{h_m b_n} \right] \quad (\text{Eqn. 13})$$

Where T_s = Temperature of the outer surface of the device

T_m = Temperature of the surrounding medium

K_n = Heat conductivity of the outer layer of the device

a_n = Radius of inner wall of the outer layer of the device

b_n = Radius of outer wall of the outer layer of the device

h_m = Radius of outer wall of the outer layer of the device

During the design process it was found that Eqn. 14 was inadequate and heat dissipation fins were needed to dissipate the excess heat created by the Sr-90TiO₃ fuel cell. During the heat dissipation fin design it was determined to place the hot junction of the thermocouple up against the layer of shielding and the cold junction up against the layer of Aluminum. To maximize the efficiency of the thermocouples used, the hot junction and cold junction were designed to have a temperature gradient of approximately 705 Kelvin.

Dealing with the Heat Using Al Encasing and Heat Dissipation Fins

In order to protect the insulation and contain the shielding while adding strength and robustness to the design, the entire fuel cell was encased in a layer of Aluminum. If the power unit is dropped or damaged, the Aluminum provides added protection from leaks or damage to the fuel cell, shielding, or the insulation layers. The Aluminum also provided increased thermal conductivity to the heat dissipation fins.

In the heat dissipation fin design it was assumed to have the outside tip of each heat dissipation fin experience convective heat transfer. An illustration of a heating fin and some of the variables used to represent the fin can be seen in Fig. 15. To describe the

heat transfer rate of each fin and heat dissipation fin efficiency, Eqn. 12a - f and 13a - b (DeWitt & Lavine 2007) were used respectively.

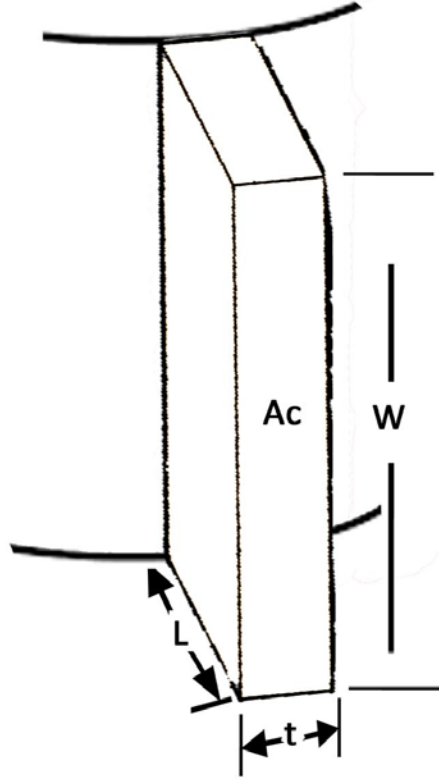


Fig. 15. Illustration of a heat dissipation fin and variables used to represent its dimensions.

$$q_f = M \frac{\sinh(mL) + (h/mk)\cosh(mL)}{\cosh(mL) + (h/mk)\sinh(mL)} \quad (\text{Eqn. 12a})$$

$$q_f = \left(15.507271 \, W/K(\theta_b) \right) \frac{0.476455073 + (0.042412829)(1.10770458)}{1.10770458 + (0.042412829)(0.476455073)} =$$

$$7.19654 \, W/K(\theta_b)$$

Where

$$M = \sqrt{hPkA_c}\theta_b \quad (\text{Eqn. 12b})$$

$$= \sqrt{(.005 \text{ W/cm}^2\text{K})(180.4 \text{ cm})(2.05 \text{ W/cm K})(130.05 \text{ cm}^2)\theta_b}$$

$$= 15.507271 \text{ W/K} (\theta_b)$$

$$\sinh \left[\left(0.05750676 \frac{1}{\text{cm}} \right) (8 \text{ cm}) \right] = 0.476455$$

$$\cosh \left[\left(0.05750676 \frac{1}{\text{cm}} \right) (8 \text{ cm}) \right] = 1.107705$$

$$\frac{h}{mk} = \frac{.005 \text{ W/cm}^2\text{K}}{\left(0.05750676 \frac{1}{\text{cm}} \right) (2.05 \text{ W/cm K})} = 0.042413$$

$$m = \sqrt{hP/kA_C} \quad (\text{Eqn. 12c})$$

$$= \sqrt{\frac{(.005 \text{ W/cm}^2\text{K})(180.4 \text{ cm})}{(2.05 \text{ W/cm K})(133.05 \text{ cm}^2)}} = 0.057507 \frac{1}{\text{cm}}$$

$$\theta_b = T_b - T_{inf} \quad (\text{Eqn. 12d})$$

$$P = 2w + 2t \quad (\text{Eqn. 12e})$$

$$= 2(88.7 \text{ cm}) + 2(1.5 \text{ cm}) = 180.4 \text{ cm}$$

$$A_C = wt = \text{Surface area of fin tip [cm}^2\text{]} \quad (\text{Eqn. 12f})$$

$$= (88.7 \text{ cm})(1.5 \text{ cm}) = 133.05 \text{ cm}^2$$

$$q_f = \text{Heat transfer rate of heat dissipation fin [W]}$$

h = heat convection coefficient of surrounding air = $.005 \text{ W/cm}^2\text{K}$

k = conductivity of material (Al) = 2.05 W/cm K

θ_b = Temperature difference between prime surface of the power unit and the

T_b = Temperature of the Prime surface

T_{inf} = Temperature of the surrounding air

$$\eta_f = \frac{q_f}{hA_f\theta_b} \quad (\text{Eqn. 13a})$$

$$= \frac{7.19654 \text{ W/K} (\theta_b)}{(.005 \text{ W/cm}^2\text{K})(1576.25 \text{ cm}^2)(\theta_b)} = 0.923593$$

Where $A_f = 2L(w + t) + wt$ = surface area of the fin [cm^2] (Eqn. 13b)

$$= 2(8 \text{ cm})[88.7 \text{ cm} + 1.5 \text{ cm}] = 1576.25 \text{ cm}^2$$

t = thickness of heat dissipation fin = 1.5 cm

L = length (or protrusion) of heat dissipation fin = 8 cm

$w = H + 2a_{outer_layer}$ = width (or height) of the heat dissipation fin
(Eqn. 13c)

$$= 72 \text{ cm} + 2(8.35 \text{ cm}) = 88.7 \text{ cm}$$

Where H = Height of fuel cell = 72cm

a_{outer_layer} = thickness of all layers outside of fuel cell = 8.35 cm

Because q_f is also a function of θ_b , the θ_b terms drop out and the fin efficiency is independent of temperature. Once the efficiency is found for one fin it was then possible to find the efficiency of the entire surface of the power unit. This is shown in Eqn. 14a (DeWitt & Lavine 2007).

$$\eta_o = 1 - \frac{N_f A_f}{A_t} (1 - \eta_f) \quad (\text{Eqn. 14a})$$

$$= 1 - \frac{(20)(1576.25 \text{ cm}^2)}{(36025.54 \text{ cm}^2)} [1 - 0.923593] = .933138$$

$$\text{Where } A_t = N A_f + A_b = \text{Total surface area of fins and prime surface } [\text{cm}^2] \quad (\text{Eqn. 14b})$$

$$A_t = (20)(1576.25 \text{ cm}^2) + 4500.543 \text{ cm}^2$$

$$= (36025.54 \text{ cm}^2)$$

$$A_b = \text{Surface area of prime surface } [\text{cm}^2]$$

$$A_b = 2\pi(R + a_{\text{outer_layer}})w - N A_c \quad (\text{Eqn. 14c})$$

$$= 2\pi(4.5 \text{ cm} + 8.35 \text{ cm})(88.7 \text{ cm}) - (20)(133.05 \text{ cm}^2) = 4500.543 \text{ cm}^2$$

$$N_f = \# \text{ of heat dissipation fins used in power unit} \quad (\text{Eqn. 14d})$$

$$= \frac{2\pi(R + a_{\text{outer_layer}})}{2.5t} - 1 = \frac{2\pi(4.5 \text{ cm} + 8.35 \text{ cm})}{2.5(1.5 \text{ cm})} - 1 = 20.53 = 20$$

Once the surface efficiency was solved it was then very simple to solve for the prime surface temperature T_b . Due to conservation of energy it can be said that the q_t equals the power output created by the Sr-90TiO3 fuel cell and thereby creating the possibility to solve for T_b . This is displayed in Eqns. 15a and 15b (DeWitt & Lavine 2007).

$$q_t = h A_t \eta_o (T_b - T_{inf}) \quad (\text{Eqn. 15a})$$

$$T_b = \frac{q_t}{hA_t\eta_o} + T_{inf} \quad (\text{Eqn. 15b})$$

$$= \frac{10626.25661 W_{th}}{(.005 W/cm^2K)(36025.54 cm^2)(.933138)} + 293.15 K = 356.3699 K$$

Where q_t = Total energy dissipation rate from power unit = 10626 Watts

After T_b was solved, it was set equal to T_2 in Eqn. 11, and propagated through to describe the temperatures at both the inside and outside of each layer all the way to the center of the fuel cell within the power unit using Eqn. 10a. The temperatures of the inside and outside of each layer, the layers' thickness, description, and heat conductivity is given in Table 6. The T_1 represents the temperature of the inside of each layer and the T_2 represents the temperature of the outside of each layer, the last T_2 equals T_b solved in the equation above.

Material Description	Material	Thickness t [cm]	Heat Conductivity (k)	T2 [K]	T1 [K]
			[W/cm*K]		
Fuel Cell	Sr-90TiO3	4.5	0.028602973	1104.907	1515.515
Protective Layer	305 Stainless Steel	0.75	0.155	1081.547	1104.907
Shielding	Uranium	0.9	0.275	1068.032	1081.547
Hot Shoe + Blanket	SiMo	0.19	1.047941028	1067.35	1068.032
Spacer + Blanket	Al2O3	0.1	0.214186401	1065.634	1067.35
Pellet and Segment + Blanket	SiGe	4	0.017263178	408.2808	1065.634
Cold Shoe + Blanket	W	0.08	0.060040605	405.2943	408.2808
Pedestal + Blanket	Cu	0.03	0.067091006	404.2973	405.2943
Compensator + Blanket	W	0.03	0.030899601	402.1388	404.2973
Electrical Connector + Blanket	Cu	0.09	0.398558244	401.6395	402.1388
Electrical Insulator + Blanket	Al2O3	0.09	0.021317578	392.3844	401.6395
Heat Shunt Inside + Blanket	Cu	0.05	0.102497299	391.322	392.3844
Heat Shunt - Compensator + Blanket	Mo	0.05	0.036251347	388.3319	391.322
Heat Shunt Legs + Blanket	Cu	0.27	0.032439305	370.5496	388.3319
Heat Shunt - Pressure Pad + Blanket	SS	0.05	0.016039767	363.9856	370.5496
Heat Shunt Outside + Blanket	Cu	0.05	0.017263178	357.9139	363.9856
Heat Fin Base	Aluminum	1.62	2.05	356.3699	357.9139

Table 6. Layer descriptions, conductivities, and temperatures of power unit.

A top-view illustration of the power unit showing each layer and labeling the temperature of the center of the fuel cell as well as the surface of each layer is given in Fig. 16.

Heat Transfer Diagram

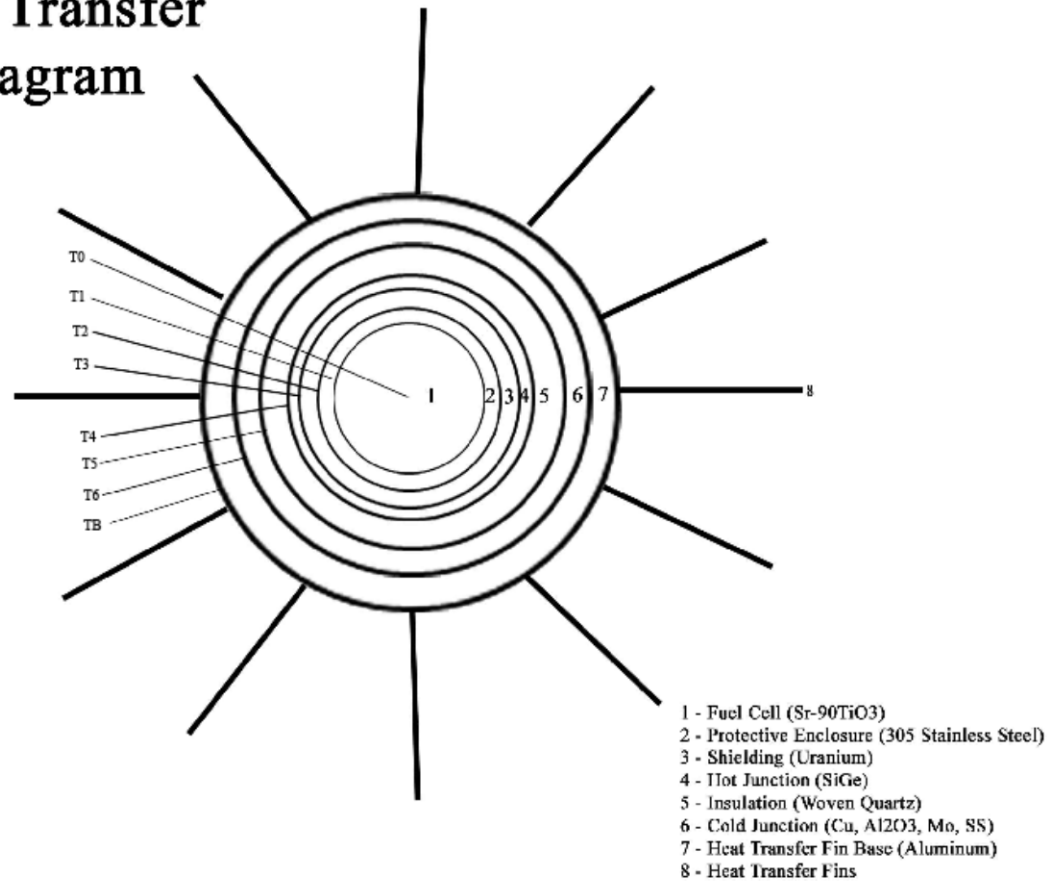


Fig. 16. Top view illustration of the layers of the power unit.

Table 6 and the corresponding illustration found in Fig. 16 is formed based on the assumption that the convection coefficient $h = .005 \text{ W/cm}^2\text{K}$, which is true if the unit is experiencing a breeze or a fan is being used to keep it cool. There is also the desire to design for the case of standing air which would change the convection coefficient to $h = .0007 \text{ W/cm}^2\text{K}$. This creates the condition of a need for a greater surface area to dissipate the heat more effectively. This design change was accomplished by increasing the length of the heat dissipation fins from 8 cm to 15cm, the thickness of the fins from

1.5 cm to 1.0 cm, and to add additional side fins that run perpendicular to the normal heat dissipation fins (To decrease the mass of the Al base the thickness of the Al base was also changed from 1.62 cm to 1.0 cm). To make these adjustments in the design Eqn. 14c had to be adjusted to account for the added surface area provided. There were also other equations made to accommodate for the side fins. These can be seen in Eqn. 16 a-c. This re-evaluation creates a different set of temperature changes between each layer and a different layout of the power unit and is given in Table 7 and Fig. 17 respectively.

$$A_t = N_f A_f + A_b + N_f S A_{sf} = \text{Total surface area of fins and prime surface } [cm^2] \quad (\text{Eqn. 16a})$$

$$= (29)(2741.26 \text{ cm}^2) + 4184.38 \text{ cm}^2 + (29)(5040.45 \text{ cm}^2) = 229853.97 \text{ cm}^2$$

$$\text{Where } S A_{sf} = (N_{sf} L_{sf})(w_{sf} + t_{sf}) = \text{Surface area added per fin due to side fins } [cm^2] \quad (\text{Eqn. 16b})$$

$$S A_{sf} = (50)(1.15 \text{ cm})(87.46 \text{ cm} + 0.2 \text{ cm}) = 5040.45 \text{ cm}^2$$

$$\begin{aligned} \text{Where } N_{sf} &= 2 \times INT \left[\frac{L}{3t_{sf}} \right] = \# \text{ of side fins per heat dissipation fin} \\ &= 2 \times INT \left[\frac{15 \text{ cm}}{3(0.2 \text{ cm})} \right] = 50 \end{aligned} \quad (\text{Eqn. 16c})$$

$$N_f = \# \text{ of heat dissipation fins} = 29$$

$$\begin{aligned} A_f &= \text{Surface area of heat dissipation fin (before side fins)} [cm^2] \\ &= 2741.26 \text{ cm}^2 \end{aligned}$$

$$A_b = \text{Surface area of power unit base } [cm^2] = 4184.38 \text{ cm}^2$$

$$L_{sf} = \text{Length of side fins} = 1.15 \text{ cm}$$

w_{sf} = Height of side fins = $w = 87.46 \text{ cm}$

t_{sf} = Width of side fins = 0.2 cm

Material Description	Material	Thickness t [cm]	Heat Conductivity (k) [W/cm*K]	T2 [K]	T1 [K]
Fuel Cell	Sr-90TiO3	4.5	0.028602973	1077.21	1487.817
Protective Layer	305 Stainless Steel	0.75	0.155	1053.849	1077.21
Shielding	Uranium	0.9	0.275	1040.335	1053.849
Hot Shoe + Blanket	SiMo	0.19	1.069323643	1039.666	1040.335
Spacer + Blanket	Al2O3	0.1	0.218784941	1037.986	1039.666
Pellet and Segment + Blanket	SiGe	4	0.017346763	383.8006	1037.986
Cold Shoe + Blanket	W	0.08	0.063148426	380.9611	383.8006
Pedestal + Blanket	Cu	0.03	0.070714361	380.0152	380.9611
Compensator + Blanket	W	0.03	0.032067238	377.9352	380.0152
Electrical Connector + Blanket	Cu	0.09	0.42494365	377.467	377.9352
Electrical Insulator + Blanket	Al2O3	0.09	0.021839679	368.4331	377.467
Heat Shunt Inside + Blanket	Cu	0.05	0.108734606	367.4316	368.4331
Heat Shunt - Compensator + Blanket	Mo	0.05	0.037840979	364.5671	367.4316
Heat Shunt Legs + Blanket	Cu	0.27	0.033767997	347.4846	364.5671
Heat Shunt - Pressure Pad + Blanket	SS	0.05	0.016205204	340.9875	347.4846
Heat Shunt Outside + Blanket	Cu	0.05	0.017346763	334.9452	340.9875
Heat Fin Base + Blanket	Aluminum	1	2.05	333.9677	334.9452

Table 7. Layer descriptions, conductivities, and temperatures of power unit designed for standing air.

Heat Transfer Diagram

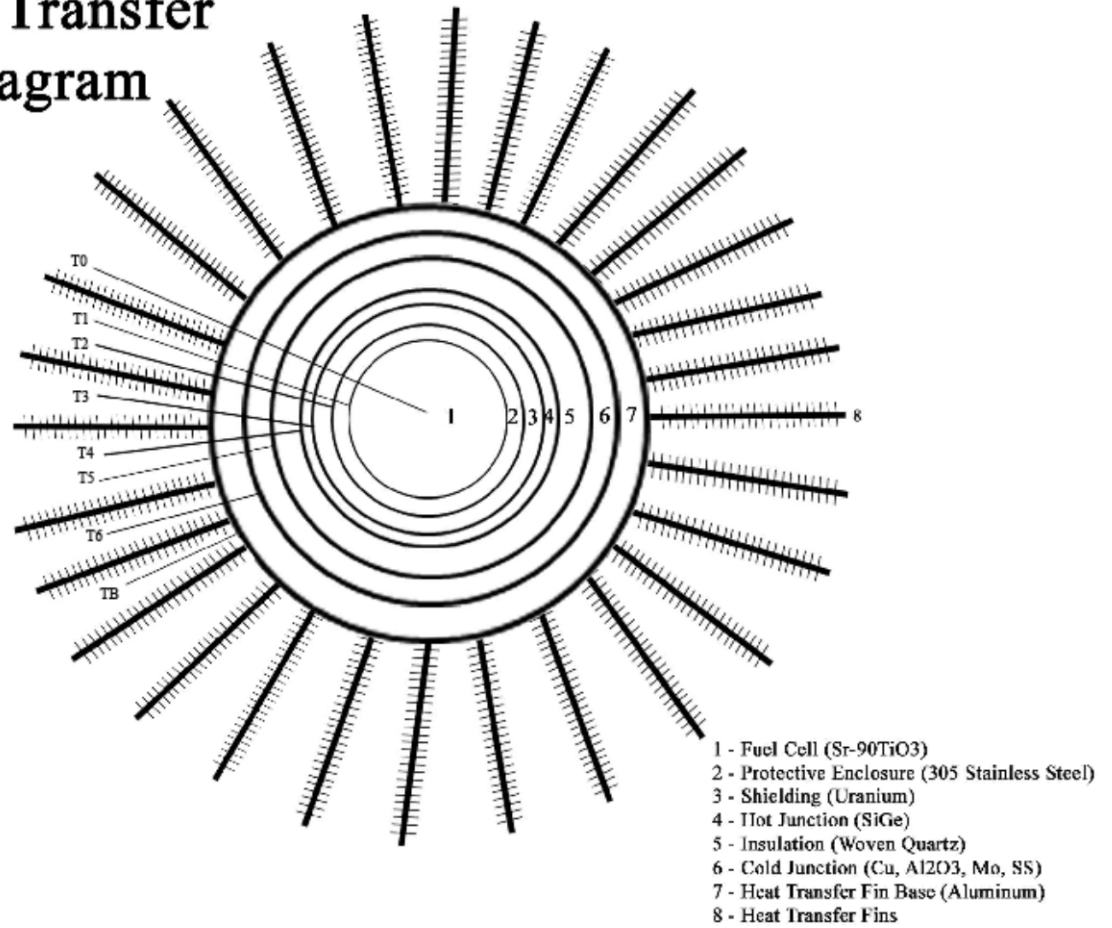


Fig. 17. Top view illustration of the layers of the power unit designed for standing air.

The process just described was used based on the assumption that the conductivity of the heat dissipation fins and base remained constant. This assumption was valid because the Biot number for each section containing one heat dissipation fin was found to be less than 0.1 in both the case for the power unit with air blowing on it and for the design where the power unit is placed in standing air. The equation for the Biot number can be seen in Eqn. 16d (DeWitt & Lavine 2007).

$$B_i = \frac{hL}{k} \quad (\text{Eqn. 16d})$$

$$= \frac{(.005 \text{ W/cm}^2 \text{ K})(8 \text{ cm})}{(2.05 \text{ W/cm K})} = 0.009846$$

Or for design for standing air

$$= \frac{(.0007 \text{ W/cm}^2 \text{ K})(15 \text{ cm})}{(2.05 \text{ W/cm K})} = 0.005122$$

Where h = Heat convection coefficient of surrounding air =
0.005 , and 0.0007 $\text{W/cm}^2 \text{ K}$

k = Conductivity of material (Al) = 2.05 W/cm K

L = Length or protrusion of heat dissipation fin = 8 and 15 cm

If the surface of the power unit is too hot, for added safety the unit could be housed in a square-steel frame and covered by a screen to prevent physical contact with the power cell as the heat dissipation fins will be very hot. The square frame will also provide ease of stacking of the power units if needed.

Possible Manufacturing Challenges

The benefits of the Sr-90TiO₃ power unit have been demonstrated but the challenges for manufacture such a device has not yet been discussed and they are considerable. The first step would obviously be to separate the Sr-90 from the spent nuclear fuel (SNF) which has been discussed but is not trivial. Then the Sr-90 would likely be compacted into one long, solid pellet, from a Sr-90TiO₃ powder within the

protective enclosure of the device and then welded shut. This task would not be simple because as was discussed earlier, the β^- particle range in air of Y-90 is nearly 30 ft. This would create the need to have any part of the fabrication that involves the Sr-90 to be within a “hot cell”. An added challenge to this is the fact that the Sr-90 and its progeny would be releasing a large amount of thermal energy within that hot cell, so special precautions would have to be made. It would likely take a customized cooling system that could dissipate the excess heat away from the hot cell without releasing any radioactive contaminants. Although this may sound like an extremely difficult task to the layman, challenges like this are met and accomplished very often within the nuclear industry.

Safety Considerations – Risks of Terrorism

Whenever nuclear material is involved there is often public concern about the risk of terrorism. More specifically, the public often wonders if it is possible for a terrorist to dismantle the device using the nuclear material and use the nuclear material to build some type of a dirty bomb or a means to assist in a terrorist attack. It is true that the contents of the fuel cell are toxic and can be fatal if enough Sr-90 is swallowed or inhaled. In fact, the annual limit of intake (ALI) for Sr-90 is 30 μCi (0.217 μg) for ingestion and 20 μCi (0.145 μg) for inhalation (U.S. NRC 2014). However, like many household products there have been clear and reasonable safeguards put in place to prevent accidental exposure to the Sr-90 within the fuel cell. If there were a terrorist attack where either the Sr-90 is separated and utilized in an explosive device or if some type of explosives were attached to the device and detonated to spread the radionuclide through the environment

to expose the population it would be ineffective. As stated by the NRC, most dirty bombs “Would not release enough radiation to kill people or cause severe illness” (U.S. NRC 2014).

Safety Considerations – Dealing with a Non-Load

While designing the Sr-90TiO₃ power unit it became obvious that there was a need to have the ability to turn off the power unit for events such as transportation of the unit or for long term storage. This need was fulfilled by designing the thermocouple to be connected in a very specific way. The thermocouple was comprised of two main sections, a hot junction and a cold junction. The hot junction was designed to be embedded within one of the layers of Mo insulation and then two wires would run from the center of each half of the hot junction and connect to the cold junction of the thermocouple which would be placed inside the Stainless steel protective layer.

This design accomplishes the ability to disconnect the array of thermocouple cold junctions from the power unit when in transit or in any situation where the need arises to disconnect the power output. But it was necessary to account for the increased heat production that would occur in the event of the cold junction connection being severed, but with an electrical efficiency of 7.5%, this was simple and was accomplished by building the unit to withstand the extra 7.5% of heat produced, whether it was used or not. Other more specific design considerations are discussed in chapter 3.

Safety Considerations – Transportation, Maintenance, and Disposal

When considering what safety requirements would need to be followed with regard to transporting Sr-90 or the Sr-90TiO₃ power units from one location to another, the same precautions that are used in nuclear fuel transportation were considered with the added precaution of dealing with the heat release of the power units. It will be necessary to provide adequate circulation to remove the approximately 10 kW of heat emanating from each device. If such a warning is ignored, the power units could overheat and end up melting and destroying themselves. With regard to durability of the transport containers, those precautions are to use casks that are able to survive what is referred to as “maximum conceivable incidents”. These incidents were the following (Shor et al 1971):

- 1) Impact of the Strontium container system equivalent to a free fall of 30 ft onto an unyielding surface.
- 2) Direct adiabatic burial (that is, engulfment in a landslide) for a period up to 48 hours.
- 3) Direct oil flame impingement for up to 2 hours a might conceivably occur in a railroad fire.
- 4) Submerged in water in a depth of 30 ft.

It would be very important to periodically check the RTG for leaks or any broken components. If the RTG were to leak and the Sr-90 was inhaled or ingested it could have deleterious health effects on the individual. For a radiation worker, the annual limit of intake (ALI) for oral ingestion and inhalation are 30 μCi and 20 μCi respectively (U.S. NRC 2014). For a member of the public it is 10% of the ALI for the radiation worker. However, with the numerous safety redundancies, it is extremely unlikely for such a

leakage to occur. Items # 1, 3, and 4 are not a problem, but #2 may need additional consideration as the power units will overheat if there are not means to dissipate the heat of the power units.

When the Sr-90TiO₃ RTG reaches the end of its life cycle, the Sr-90 will have completely decayed to Zr-90, which is a stable and completely non-toxic substance. However, before all of the Sr-90 has decayed the Sr-90TiO₃ RTG will eventually become nearly useless in terms of power production but will still contain enough Sr-90 to pose a health risk if one were so inclined to destroy/open the device to extract the Sr-90. Because of this it may be recommended to have a national repository for the Sr-90TiO₃ RTGs that are approaching their lifecycle. At the request of the Russians, the Norwegian government has already done extensive work on setting up registries, and feasibility studies on what constitutes an ideal location for a repository and it would be recommended to follow their recommendations (Sneve et al 2007).

Chapter 3 - Specific Design

Optimization of Surface Area to Maximize Amount of Thermocouples Used

With the thermal power output per unit gram at the end of the operational period of the power device determined, to find the mass required to perform the desired electrical output one would combine the overall efficiency which includes the efficiency of the thermocouples used as well as any other losses. This is shown in Eqn. 17a.

$$M_{t_final} = \frac{P_e}{(P_{th_p_t_final})(\epsilon)} \quad (\text{Eqn. 17a})$$
$$= \frac{300W_e}{(0.220480494 \text{ W/g})(0.058483319)} = 23,265.9 \text{ g Sr} - 90\text{TiO}_3$$

Where M_{t_final} = Mass of Sr-90TiO₃ fuel required to provide desired electrical power output for the operational life.

P_e = Desired electrical power output of power device at the end of the operational life = 300 We

ϵ = Overall efficiency of power unit = 0.058483

Assuming a zero failure rate of thermocouples installed within the power unit, the only other loss exists due to the fact that the thermocouples may not cover the entire surface area of the device and therefore some of the heat produced by the power unit will escape without being used to create electricity. To maximize the overall efficiency of the power unit it was necessary to maximize the percentage of the heat that actually passed through the thermocouples. To accomplish this, it was assumed that the hot shoe of each thermocouple was placed 2 mm apart (making it 2.49cm x 2.49 squares) from one another in an array surrounding the depleted U shielding. There was also an array of

thermocouples placed over the depleted U shielding on the top and the bottom of the power unit. This is illustrated in Fig. 18 below.

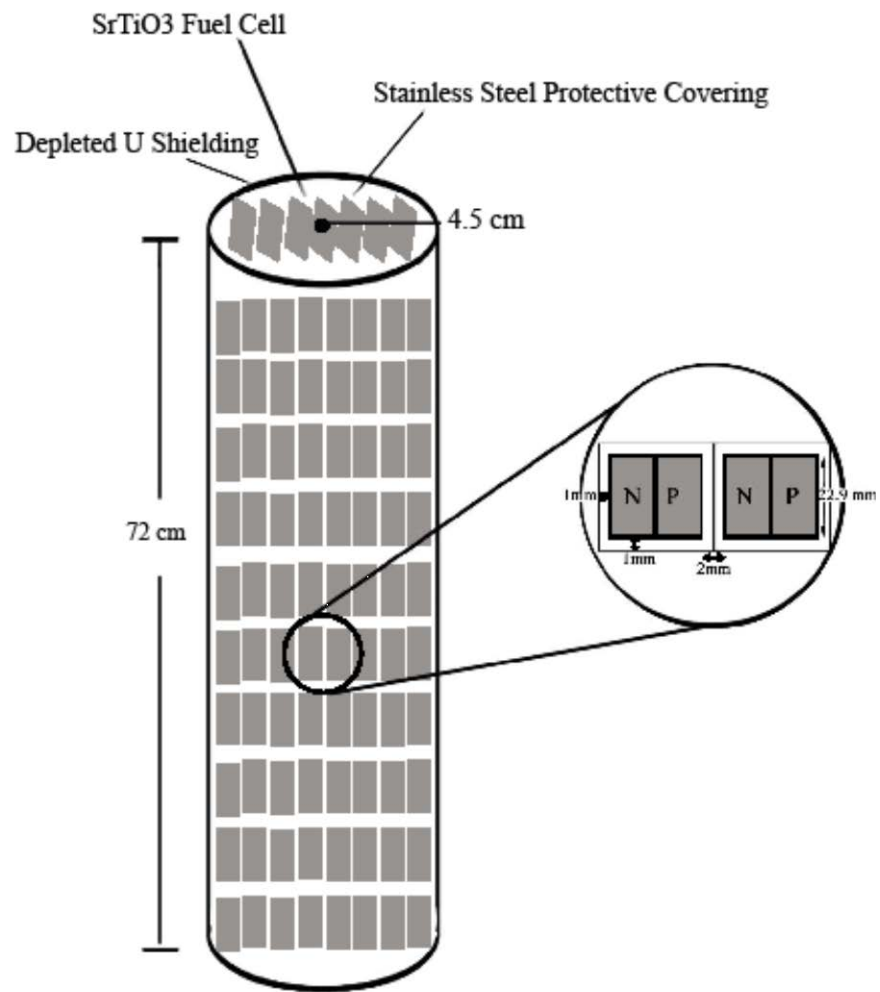


Fig. 18. Illustration of array of the thermocouple hot junctions on surface of shielded fuel cell.

To calculate the surface area available for the thermocouple arrays the following equations were used:

Surface Area for the Side of the Shielded Fuel Cell Cylinder

$$SA_{side} = 2\pi(R + a_{shield})(H + 2a_{shield}) \quad (\text{Eqn. 17b})$$

$$= 2\pi(4.5 \text{ cm} + 1.65 \text{ cm})(72 \text{ cm} + 2(1.65 \text{ cm})) = 2909.7117 \text{ cm}^2$$

Where SA_{side} = Surface area of side of shielded fuel cell = 2909.7117 cm^2

R = Radius of fuel cell = 4.5 cm

a_{shield} = thickness of protective enclosure and shielding = 1.65 cm

H = Height of the fuel cell = 72.0 cm

The next step was to calculate the number of thermocouples that could fit within the side of the shielded cylinder. To accomplish this, the size of the thermocouple array had to be determined and is shown in Eqn. 17c for the width and Eqn. 17d for the height.

$$P_{shield} = 2\pi(R + a_{shield}) \quad (\text{Eqn. 17c})$$

$$= 2\pi(4.5 \text{ cm} + 1.65 \text{ cm}) = 38.641590 \text{ cm}$$

Where P_{shield} = Perimeter (width) of side of shielded fuel cell = 38.641590 cm

R = Radius of fuel cell = 4.5 cm

a_{shield} = thickness of protective enclosure and shielding = 1.65 cm

$$H_{shield} = H + 2a_{shield} \quad (\text{Eqn. 17d})$$

$$= 72 \text{ cm} + 2(1.65 \text{ cm}) = 77.3 \text{ cm}$$

Where H_{shield} = Height of fuel cell plus protective enclosure and shielding = 77.3 cm

H = Height of fuel cell = 72 cm

a_{shield} = thickness of protective enclosure and shielding = 1.65 cm

To solve for the number of thermocouples that would fit on the side of the shielded fuel cylinder it was necessary to divide Eqn. 17c and Eqn. 17d by 2.49 cm, take the integer value of the results and multiply them together. This is shown in Eqn. 17e.

$$N_{th_side} = \left(\text{int} \left(\frac{P_{shield}}{L_{th_g}} \right) \right) \left(\text{int} \left(\frac{H_{shield}}{L_{th_g}} \right) \right) \quad (\text{Eqn. 17e})$$

$$= \left(\text{int} \left(\frac{38.6416 \text{ cm}}{2.49 \text{ cm}} \right) \right) \left(\text{int} \left(\frac{77.3 \text{ cm}}{2.49 \text{ cm}} \right) \right)$$

$$= (15)(31) = 450$$

Where N_{th_side} = Number of thermocouples able to fit on the vertical side of the shielded fuel cell = 450 thermocouples

P_{shield} = Perimeter (width) of side of shielded fuel cell = 38.6416 cm

H_{shield} = Height of fuel cell plus protective enclosure and shielding = 77.3 cm

Maximizing the Number of Thermocouples on the Shielded Fuel Cell Top and Bottom

The first step in calculating the number of thermocouples that were used on the top and bottom of the shielded fuel was to calculate the surface area, which is shown in Eqn. 17f.

$$\begin{aligned} SA_{top_bottom} &= 2\pi(R + a_{shield})^2 & (\text{Eqn. 17f}) \\ &= 2\pi(4.5 \text{ cm} + 1.65 \text{ cm})^2 = 237.646 \text{ cm}^2 \end{aligned}$$

Where SA_{top_bottom} = Surface area of top and bottom of shielded fuel cell = 237.646 cm^2

R = Radius of fuel cell = 4.5 cm

a_{shield} = thickness of protective enclosure and shielding = 1.65 cm

Then it was necessary to come up with a way to fit the maximum amount of $2.49 \text{ cm}^2 \times 2.49 \text{ cm}^2$ squares within circles formed by the top and bottom of the shielded fuel cell. To accomplish this an algorithm was found, using a visual basic macro within Excel (MathStackExchange.com 2014). While using the program, it was found that it would be possible to fit 9 $2.49 \text{ cm}^2 \times 2.49 \text{ cm}^2$ squares within the circle of radius 4.5 cm (see appendix A). So with the top and bottom being used it brings 18 thermocouples (9 on top + 9 on bottom) that were able to fit on the surface of the top and bottom of the shielded fuel cell.

Once the number of thermocouples that were able to fit on the shielded fuel cell, to find the percentage of surface area covered it was necessary to multiply the number of

thermocouples with the surface area of each thermocouple, then divide this value by the total surface area. This is shown in Eqn. 17g.

$$SA_{percent} = \frac{(N_{th_side} + N_{top_bottom})(SA_{th})}{(SA_{side}) + (SA_{top_bottom})} \quad (\text{Eqn. 17g})$$

$$= \frac{(450 + 18)(2.29 \text{ cm})^2}{(2909.7117 \text{ cm}^2) + (237.6457763 \text{ cm}^2)} = 0.779778$$

Where $SA_{percent}$ = Percentage of the surface area of the shielded fuel cell covered by thermocouples = 0.779778

N_{th_side} = Number of thermocouples on the side of the shielded fuel cell = 450

N_{top_bottom} = Number of thermocouples on the top and bottom of the shielded fuel cell = 18

SA_{th} = Surface area of a single thermocouple = 5.2441 cm^2

SA_{side} = Surface area of side of shielded fuel cell = 2909.717 cm^2

SA_{top_bottom} = Surface area of top and bottom of shielded fuel cell = 237.646 cm^2

Once the percent of the surface area of the shielded fuel cell was determined it was then necessary to calculate the overall efficiency of the power unit and is described in Eqn 17h.

$$\varepsilon = SA_{percent} \varepsilon_{th} \quad (\text{Eqn. 17h})$$

$$= (0.779777581)(.075) = 0.058483$$

Where ε = Overall efficiency of power unit

ε_{th} = Efficiency of the Thermocouples used = 0.075

$SA_{percent}$ = Percentage of the surface area covered by the thermocouples
= 0.779778

Attempting to achieve 7% efficiency

In order to get the 7% power efficiency from the thermocouples that were used in RTGs such as Galileo, Ulysses, and others it was necessary to have the specific temperature of 1273 Kelvin at the hot junction and a 566 Kelvin at the cold junction of each thermocouple used within the device or a temperature difference of 705 K. To accomplish this several layers of various materials, each with their individual thermal conductivities, were used to conduct the heat produced by the fuel cell to the outside. The many layers of Mo insulation were used to raise the temperature at the hot junction of the thermocouples to the appropriate value. In this design, the temperatures of the hot and cold junctions were 1040 K and 335 K respectively. 7% was not achieved but that was not due to any fault with the thermocouples, but the amount of the surface area of the fuel cell that was covered by the thermocouples which resulted in an overall efficiency of 5.85%.

Appropriate Shielding for a Product Sold to the Public

Because the public knowledge of nuclear technology is often misunderstood or feared, it was desirable to provide shielding that was so effective that the dose received by

an individual standing by the power unit would receive substantially less radiation than background. This was accomplished primarily by using depleted Uranium (U) as the shielding material. It was so effective that the final dose rate that would be received by an individual touching the prime surface of the power unit was 0.44×10^{-6} Rems/hr or 3.9 mRem/yr. A person living at sea level receives approximately 293 mRem/yr from natural radiation (EPA.org). The dose received per year by the power unit is less than two orders of magnitude of dose than a person would receive if they was touching the power unit constantly for an entire year! This was purposefully designed this way to help to calm any fears that the public may have of using a device that utilizes nuclear energy. Of course, neither of such small doses have ever shown to be detrimental to the health of a person.

Not Destroying Itself with no Load

Preventing the power unit from destroying itself during a “No-Load” case was accomplished by first creating the situation where there was a method of turning of the power even though there is no turning off the radiation. This was done by disconnecting the hot and cold junctions of the thermocouple and placing a switch in-between them. This switch was created by using thin sheets with metal contacts that could be slid between the hot junction and the cold junction. The default position of the “switch-ring” is in the “off” position because the sheets need not be installed until the power unit is ready to be turned on. When the power of the Sr-90TiO₃ power unit is turned on the hot and cold junctions of the thermocouples are connected throughout the device. The cold junction of the thermocouples is inside the protective layer of Aluminum.

The design would include thermocouples in an array covering the entire side of the cylindrical power unit. At the location of the cold junction there would be a movable rod at the position of each vertical array of thermocouples that would alternate between an insulator and a conductor. When the insulator is in contact with the cold junction of the thermocouple the connection to the hot junction would be broken and the power unit would be in the “Off” position. When the conductor is in contact with the cold junction of the thermocouple the connection to the hot junction would be restored and the power unit would be in the “On” position. These “switch rods” would be connected at the top and bottom of the power unit forming a “switch rod ring”. The initial position of the switch rods would be in the off position. An illustration of this configuration can be seen in Fig. 19.

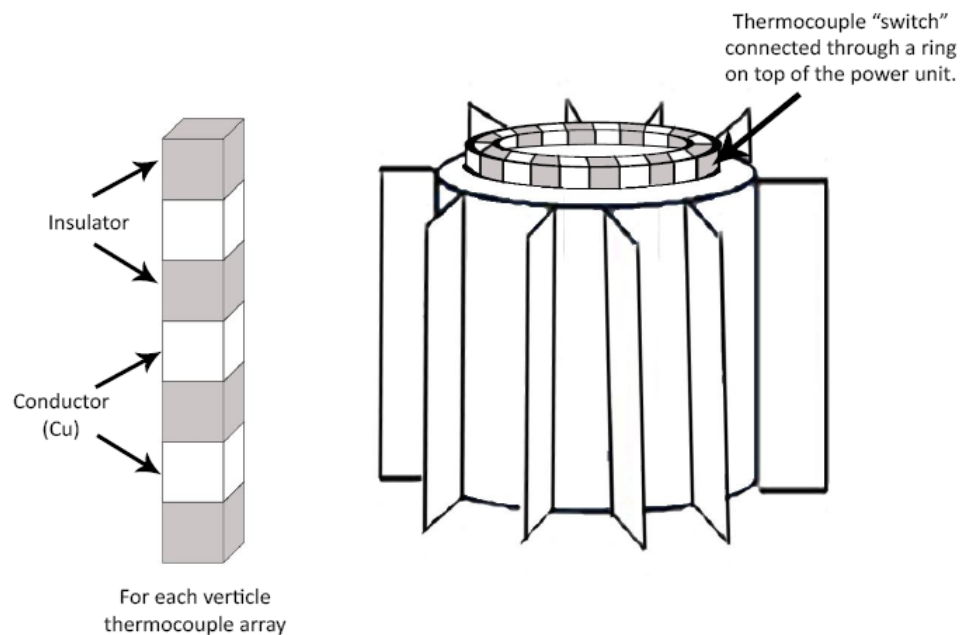


Fig. 19. Illustration of a single “switch rod” (left) and the “switch rod ring” (right) installed (in off position).

An illustration of a hot and cold junction for a single thermocouple can be seen in Fig. 20. An illustrated close-up view of the top layer of two thermocouples in the Sr-90TiO₃ power unit is given in Fig. 21. Also, each layer of the power unit is displayed in an “X-Ray” view with the thermocouple components and is included in Fig. 22.

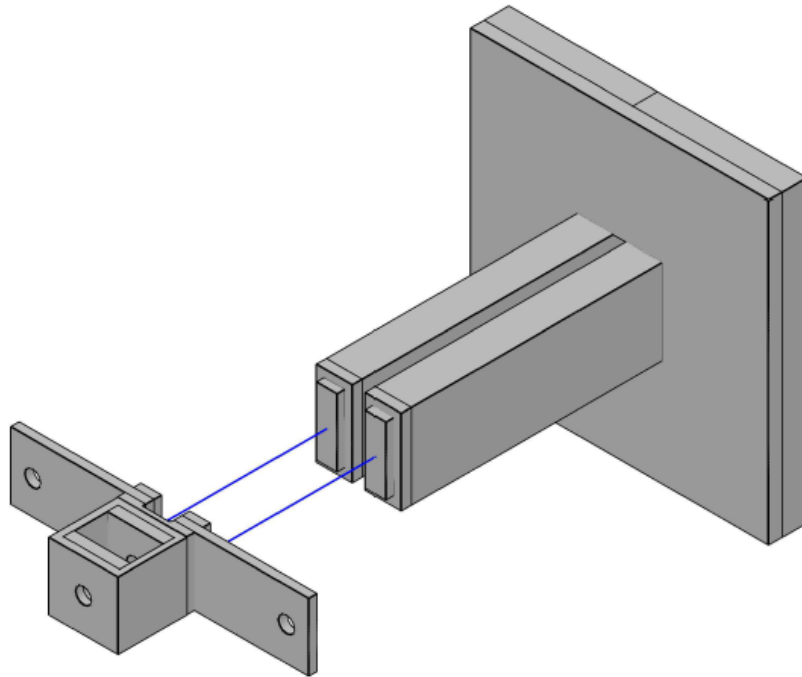


Figure 20. Illustration of the hot and cold junction of a single thermocouple.

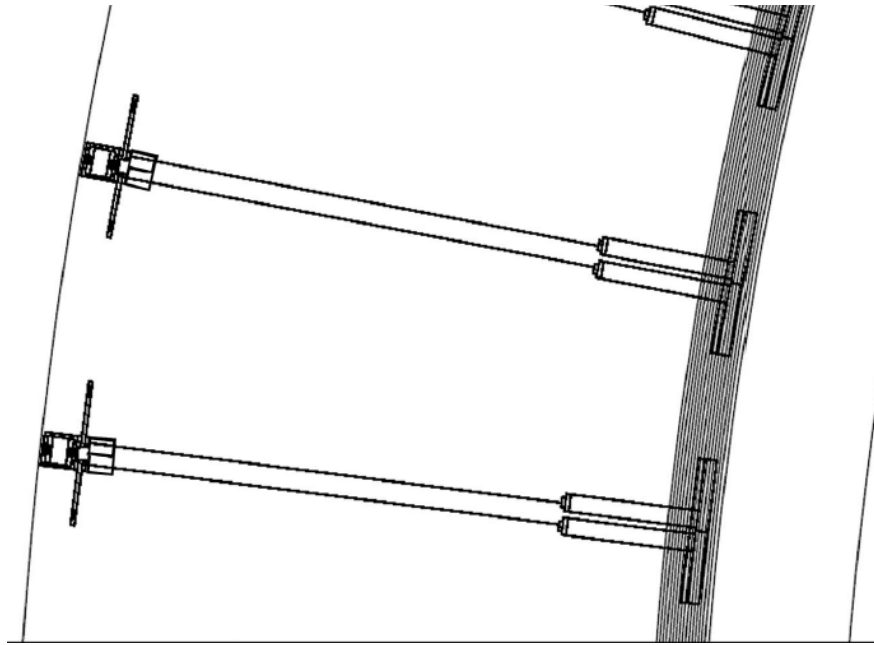


Fig. 21. Top view of hot and cold thermocouple junctions connected.

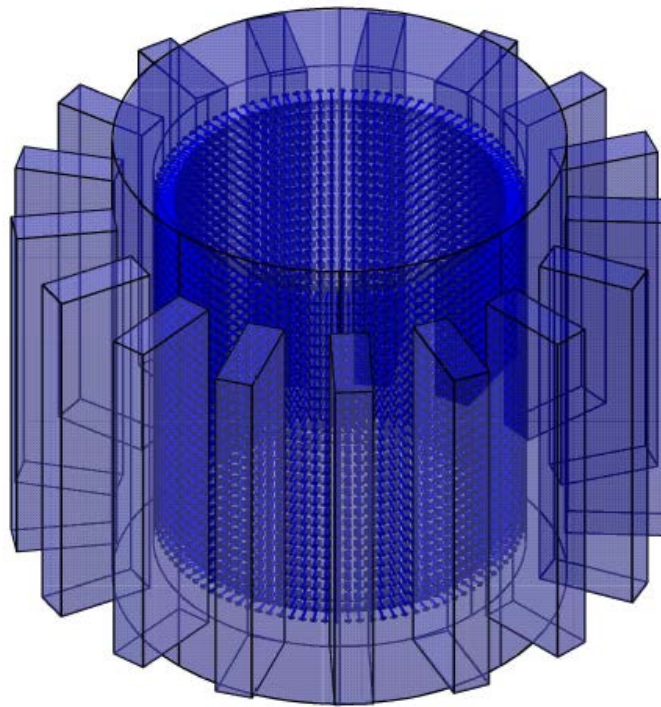


Fig. 22. “X-Ray” view of Sr-90TiO3 power unit and its components.

During this “No-Load” condition it was important to realize that the materials within the power unit itself would need to accept the higher internal temperatures that will occur when the extra heat that was not converted into electricity, so the melting points of the materials had to be considered. The melting points of the materials used and considered can be seen in Table 8. As seen in the table, Pb was considered to be used as the shielding material, but because the melting point of Pb is so low, depleted U was used. All other material melting points were within the required range given by the design.

Melting Points of Considered Materials

Material	Material Melting Point		
	Kelvin	Celcius	Farenheight
Tungsten (W)	3695.15	3422	6191
Molybdenum (Mo)	2916.15	2623	4789.4
Sr-90TiO3	2373.15	2080	3812
Al2O3	2345.15	2072	3762
Woven Quartz	1923.15	1650	3002
Iron (Fe)	1831.15	1538	2836.4
304 Stainless (SS)	1718.15	1425	2633
SiGe	1588.15	1295	2399
Uranium (U)	1425.15	1132	2105.6
Fiberglass - Melts	1414.15	1121	2085.8
Copper (Cu)	1357.77	1084.62	1984.316
Fiberglass - Softens	1139.15	846	1590.8
Aluminum (Al)	953.15	660	1256
Lead (Pb)	620.61	327.46	657.428

Table 8. Melting points of considered materials.

Adding Side Fins to Design for Power Unit in Standing Air

In order to have the power unit have the ability to remain within the proper operating temperature there was a need for additional surface area to transfer all of the excess heat, which was accomplished by adding additional heat dissipation fins called side fins. The side fins are perpendicular to the normal heat dissipation fins. The decision of how many side fins were needed, and the desired dimensions of each side fin was determined by altering Eqn. 14b. to get the necessary surface area to accommodate the increased heat transfer, which is described in Eqns. 18 a – c. A 3-D rendition of the power unit, designed for use under a constant breeze and for the case of standing air was made and can be seen in Fig. 23 and Fig. 24 respectively.

$$A_{tot} = N_f A_f + A_b + N_f S A_{sf} \quad (\text{Eqn. 18a})$$

Where A_{tot} = Total surface area of the power unit

N_f = # of heat dissipation fins

A_f = Surface area of the heat dissipation fins (not counting side fins)

A_b = Surface area of prime surface (Eqn. 14c)

$$S A_{sf} = 2 N_{sf} L_{sf} [w_{sf} + t_{sf}] \quad (\text{Eqn. 18b})$$

= Total added surface area due to side fins per heat dissipation fin

L_{sf} = Length (or protrusion) of side fin

w_{sf} = Width (or height) of side fin

t_{sf} = Thickness of side fin

$$\text{Where } N_{sf} = 2 \text{int} \left(\frac{L}{3t_{sf}} \right) \quad (\text{Eqn. 18c})$$

= # of side fins per heat dissipation fin

L = Length (or protrusion) of heat dissipation fin

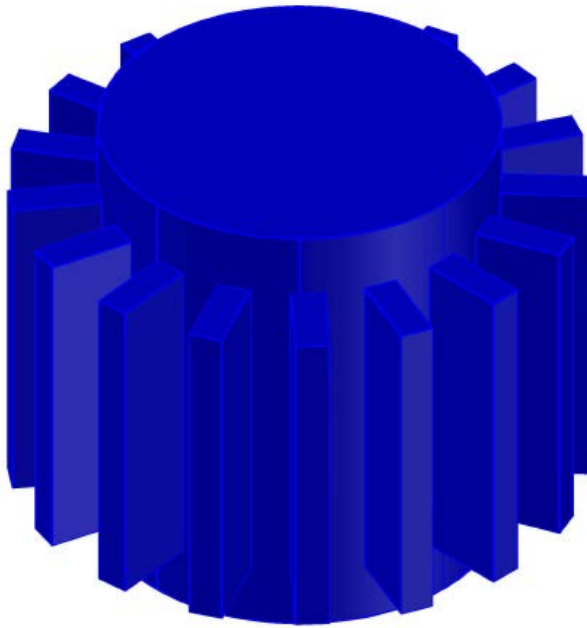


Fig. 23. 3-D rendition of Sr-90TiO3 power unit (designed to be maintained under a constant breeze).

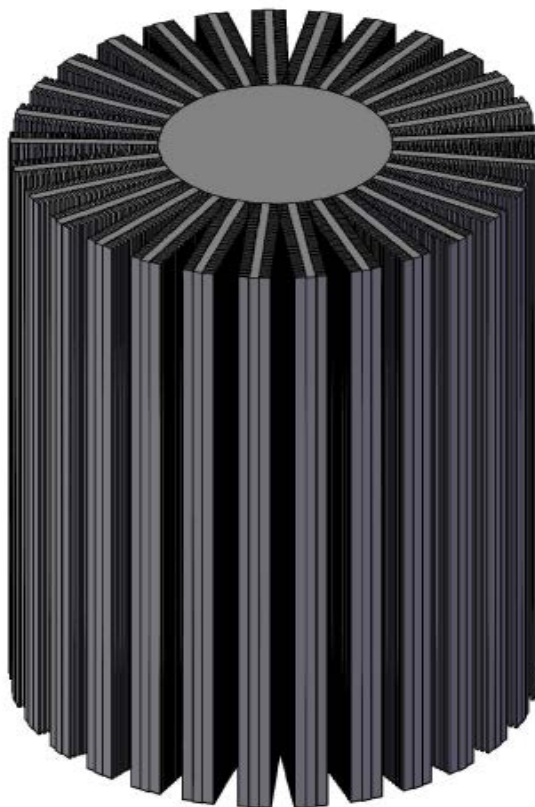


Fig. 24. 3-D rendition of Sr-90TiO3 power unit (designed to be in standing air).

Chapter 4 - Marketing

Possible Uses of the Technology

The market for the Sr-90TiO₃ power unit could potentially supplement the sector of the solar power market that focuses on low power, long term, and stable power usage. Some examples include scientific data gathering instruments such as weather tracking. The Sr-90TiO₃ RTG may be an advantage over less robust designs performed by solar panels. An example in agriculture for the Sr-90-TiO₃ RTG would be using it to power an electric fence. Another use could be to power a light house. This would be particularly useful for a lighthouse in a remote area that gets very few visitors. Another possible application would be to have the power unit used for portable power at extremely remote locations such as at the arctic or Antarctica for applications such as power for research stations or other relatively low power needs.

Another application that would be very useful would be as a back-up power system for highly sensitive or high security data. If it is absolutely necessary to guarantee that the power will be on to store a company's data, or to make sure that a network server always has power, the Sr-90TiO₃ RTG may be the answer. Another application for the Sr-90TiO₃ RTG could be used on naval vessels in applications that are necessary to have a source of reliable power such as the communication system. There are also implications of several possible military applications. For example, one way to use the Sr-90TiO₃ RTG is to provide quick and easy setup of a power source for a military base. If more power is needed than one Sr-90TiO₃ can provide then multiple Sr-90TiO₃ sources can be brought together and connected to the same system. When the base is no longer needed,

one only needs to disconnect the unit and carry it to the next location. Another possible military application of the Sr-90TiO₃ RTG is to provide enough power for the necessary surveillance equipment such as video and audio recording devices that can be placed in areas of high interest that may not access to power. All the while containing enough power for a remote transmitting device to provide the surveillance Intel in real-time.

Ideal Application

There are many ways that the Sr-90TiO₃ RTG can be useful but the area that it may be the most useful may be to power housing, particularly in remote areas. The ability to have a 300 Watt power unit that will last 30+ years and weighs light enough to eliminate the need for heavy equipment to move the power unit can be very useful. This unit would especially be useful to provide power in remote areas such as a log cabin in Alaska. Because the cabin may not be constantly using the full power it would also be necessary to include a charge controller and battery pack, similar to what is currently used in a solar power residential power unit. An illustration of a system using the Sr-90TiO₃ power unit producing both DC and AC power is given in Fig. 25. If more power is desired, one can simply integrate more Sr-90TiO₃ power units into the system for either DC or an AC power system. Because there are greater power losses in an AC power system one would typically use an AC power system with the increased power provided by the Sr-90TiO₃ power units which is illustrated in Fig. 26.

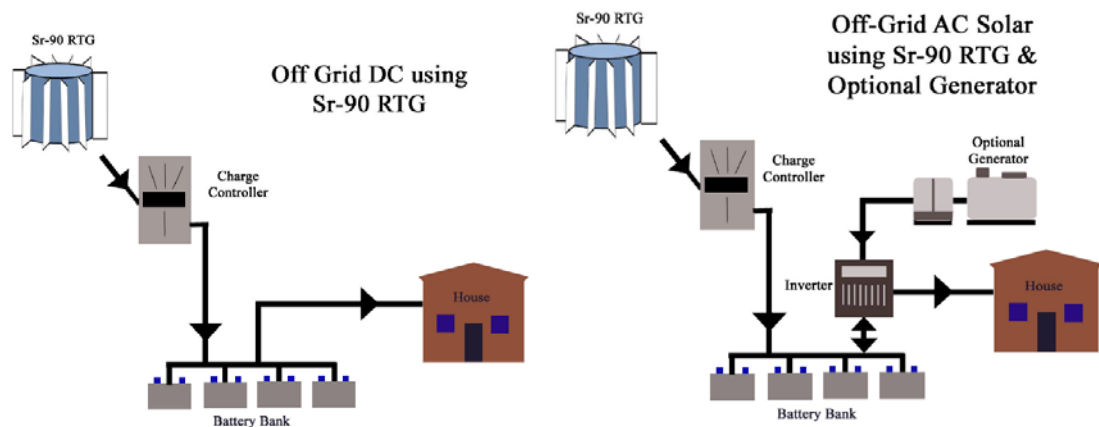


Fig. 25. Illustration of DC (left) and AC (right) remote power system using a single Sr-90TiO3 power unit.

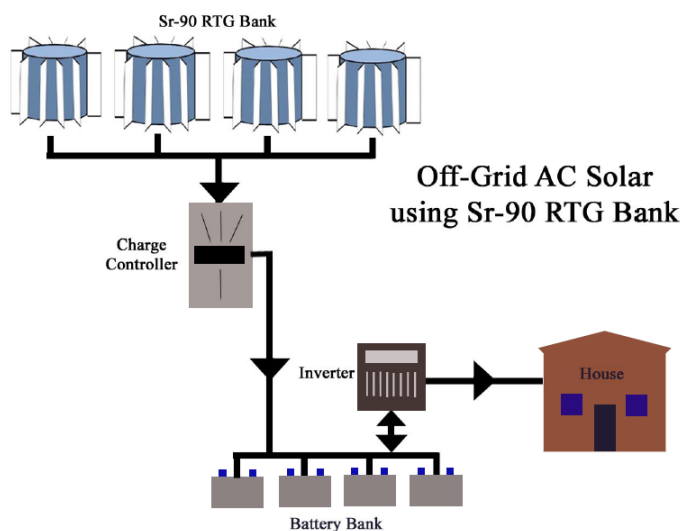


Fig. 26. Illustration of AC remote power system using multiple Sr-90TiO3 power units.

Future Work

When looking at possible improvements to the Sr-90TiO3 RTG, two items came to mind. The first item would be to look into more effective thermocouple materials that can

be more efficient and be just as robust and reliable as the thermocouples that were chosen to be in this design. There are other materials that can produce a higher energy conversion efficiency, in fact some are as high as 26% (El-Genk 2007), but don't yet have the track record of reliability as the thermocouples used in this design. It would be worthwhile to investigate and test these materials.

The second item that would be valuable to do in order to further this work would be to actually build a prototype. There would be several challenges to overcome and many lessons to learn and would give insight into what it would take to mass produce Sr-90TiO₃ RTG power units and the monetary costs required to accomplish such a task. Although the actual monetary cost of manufacturing and fabricating the Sr-90 RTG was never reported specifically by Oak Ridge, what they did say was that the initial capital cost was high, but when the cost per Watt produced over the RTG's lifetime was calculated, it was said to be comparable to other remote power system prices.

Chapter 5 – Conclusion

A power unit using the radionuclide Sr-90 was designed to produce 300 W of electricity after 30 years of use (621 W initially). The power unit's fuel cell consists of Sr-90TiO₃ because the chemical, thermal, and physical properties were ideal compared to other Sr-90 compounds. A power unit was designed for the case of the power unit to be standing under a breeze (or the use of cooling fans) and in the case of the power unit not experiencing any external forced convection. The specifications for the latter case are described here. The unit itself weighs approximately 582.5 Lbs (108.7 Lbs are depleted Uranium) and has 29 heat dissipation fins that are 15.0 cm x 1.0 cm x 87.46 cm. Each heat dissipation fin has 50 side fins that are 1.15 cm x 0.2 cm x 87.46 cm. The fuel cell has a cylindrical shape and a radius of 4.5 cm and a height of 72.0 cm. The dose rate that an individual would receive touching the prime surface of the power unit is 0.44×10^{-6} Rem/hr (0.0044 μ Gy/hr). The Sr-90TiO₃ power unit was designed to be fully functional without any moving parts and provides a sustainable use for an abundant fission product, as well as an effective way to use some of the depleted Uranium that is stockpiled throughout the United States.

References

1. Gary L. Bennet and James J. Lombardo (formerly of the U.S. Department of Energy and NASA), Richard J. Hemler and Gil Silverman (formerly of Lockheed-Martin Space Systems Company), C.W. Witmore (formerly of General Electric Company), Wayne R. Amos and E. W. Johnson (formerly of Mound Laboratory), Alfred Schock (formerly of Orbital Sciences Corporation), Roy W. Zocher and Thomas K. Keenan (formerly of Los Alamos National Laboratory), James C. Hagan (formerly of Johns Hopkins University Applied Physics Laboratory), Richard W. Englehart (U.S. Department of Energy). Mission of Daring: The General-Purpose Heat Source Radioisotope Thermoelectric Generator. 4th International Energy Conversion Engineering Conference and Exhibit. AIAA 2006 – 4096. June 2006.
2. Jordi Bruno, Rodney C. Ewing. Spent Nuclear Fuel. Elements. December 2006, Vol. 2, pp. 343 – 349.
3. Matthew Bun, Steve Fetter, John P. Holdren, Bob van der Zwaan. The Economics of Reprocessing Vs. Direct Disposal of Spent Nuclear Fuel. Belfer Center for Science and International Affairs, John f. Kennedy School of Government. December 2003.
4. Bureau of Radiological Health. Radiological Health Handbook. U.S. Department of Health, Education, and Welfare. January 1970. Pgs. 137 – 139.
5. Herman Cember, Thomas Johnson. Introduction to Health Physics. 4th Edition. McGraw Hill. 2009. Pg. 147 Equation 5.5.
6. Incropera DeWitt, Bergmann Lavine. Fundamentals of Heat and Mass Transfer. Wiley 2007. Chapter 3, pgs. 144.

7. Mohamed S. El-Genk. Space nuclear reactor power system concepts with static and dynamic energy conversion. Institute for Space Nuclear Power Studies. Chemical and Nuclear Engineering Department, University of New Mexico, Albuquerque. Energy Conversion and Management 49 (2008) 402 – 411.
8. S. Glasstone, A. Sesonske. Nuclear Reactor Engineering. 3rd Edition. XanEdu Publishing. 2010. Pgs. 648 – 650.
9. Frank N. von Hippel. Plutonium and Reprocessing of Spent Nuclear Fuel. Science, Volume 293, Number 5539, Issue of September 2001, pp. 2397 – 2398.
10. How much electricity do an American home use? U.S. Energy Information Administration, Frequently asked questions.
<http://www.eia.gov/tools/faqs/faq.cfm?id=97&t=3>
11. ICRP Committee. Limits for Intakes for Radiation Workers. International Committee for Radiation Protection. 1979
12. R.G. Jaeger, E.P. Blizard, A.B. Chilton, M. Grotenhuis, A. Honig, Th. A. Jaeger, H. H. Eisenlohr. Engineering Compendium on Radiation Shielding. Volume I Shielding Fundamentals and Methods. Springer-Verlag 1968. Pgs. 384, 415.
13. Thomas E. Johnson, Brian K. Birky. Health Physics and Radiological Health. Lippincot Williams & Wilkins. Baltimore MD. 2012. Pg. 49
14. John R. LaMarsh, Anthony J. Baratta. Introduction to Nuclear Engineering. 3rd Edition. Prentice Hall Inc. 2001. Pg. 552.

15. Robert G. Lange, Wade P. Carroll. Review of recent advances of radioisotope power systems. *Energy Conversion and Management* 49 (2008), pp 393 – 401.
16. James E. Martin. *Physics for Radiation Protection*. Wiley-BCH, Second Edition. 2011. Pg. 369.
17. <http://math.stackexchange.com/questions/606002/number-of-squares-in-a-circle>
18. National Institute of Standards and Technology.
<http://physics.nist.gov/PhysRefData/XrayMassCoef/ElemTab/z82.html>
19. Sneve M.K, Reka V. Upgrading the Regulatory Framework of the Russian Federation of the Safe Decommissioning and Disposal of Radioisotope Thermoelectric Generators. *Stralever Rapport* 2007:5. Osteras: Norwegian Radiation Protection Authority, 2007.
20. Solar Facts. How much of your DC power comes out as AC Power?
<http://www.solar-facts.com/inverters/inverter-efficiency.php> 2014.
21. Roberta Shor, Robert H. Lafferty, Jr., P. S. Baker. Strontium-90 Heat Sources. Isotopes Information Center, Oak Ridge National Laboratory. May 1971.
22. Terry Todd, Spent Nuclear Fuel Reprocessing. Nuclear Regulatory Commission Seminar, Idaho National Labs, March 2008.

Appendix A – Excel 2007 Code used to solve the # of squares in a circle

Option Explicit

Sub addShapeDemo()

Dim shape As Excel.shape

Dim x As Single

Dim y As Single

Dim mx As Single

Dim my As Single

Dim col As Integer

Dim cols As Integer

Dim row As Integer

Dim rows As Integer

Dim d2 As Single

Dim xMin As Single

Dim yMin As Single

Dim squares As Integer

Const radius = 4.5 ' results in 341 squares

Const a = 2.49 ' square dimension

mx = 800 ' center of the circle

my = 800

' clean our sheet from previous drawings

On Error Resume Next

ActiveSheet.DrawingObjects.Delete

' draw the circle nicely colored

Set shape = ActiveSheet.Shapes.AddShape(msoShapeOval, Left:=mx - radius, _

Top:=my - radius, Width:=2 * radius, _

Height:=2 * radius)

shape.Select

Selection.ShapeRange.Fill.Visible = msoFalse

With Selection.ShapeRange.Line

.ForeColor.RGB = RGB(255, 0, 0)

.Weight = 2.25

End With

With Selection.ShapeRange.Fill

.Visible = msoTrue

.ForeColor.RGB = RGB(255, 255, 0)

End With

' draw the boxes

rows = (2 * radius) \ a

yMin = my - a * 0.5 * ((2 * rows) \ 2)

For row = 1 To rows

' find out how many columns to place

' outer corner must stay within our circle

y = yMin + (row - 1) * a

If row <= rows \ 2 Then

```

        cols = (2# * ((radius * radius - (y - my) * (y - my)) ^ 0.5)) \ a
Else
        cols = (2# * ((radius * radius - (y - my + a) * (y - my + a)) ^ 0.5)) \ a
End If

' center the line
xMin = mx - a * 0.5 * ((2 * cols) \ 2)

For col = 1 To cols
        x = xMin + (col - 1) * a
        ActiveSheet.Shapes.AddShape msoShapeRectangle, Left:=x, _
                Top:=y, Width:=a, Height:=a
        squares = squares + 1
Next col
Next row
MsgBox squares & " squares"
End Sub

```